Available online at www.sciencedirect.com
SCIENCE DIRECT®
Physics Reports 392 (2004) 279–319
PHYSICS REPORTS
www.elsevier.com/locate/physrep

Lagrangian fluid description with simple applications in compressible plasma and gas dynamics

Hans Schamel

Physikalisches Institut, Universität Bayreuth, D-95440 Bayreuth, Germany

Accepted 2 December 2003
editor: D.L. Mills

Abstract

The Lagrangian fluid description, in which the dynamics of fluids is formulated in terms of trajectories of fluid elements, not only presents an alternative to the more common Eulerian description but has its own merits and advantages. This aspect, which seems to be not fully explored yet, is getting increasing attention in fluid dynamics and related areas as Lagrangian codes and experimental techniques are developed utilizing the Lagrangian point of view with the ultimate goal of a deeper understanding of flow dynamics. In this tutorial review we report on recent progress made in the analysis of compressible, more or less perfect flows such as plasmas and dilute gases. The equations of motion are exploited to get further insight into the formation and evolution of coherent structures, which often exhibit a singular or collapse type behavior occurring in finite time. It is argued that this technique of solution has a broad applicability due to the simplicity and generality of equations used.

The focus is on four different topics, the physics of which being governed by simple fluid equations subject to initial and/or boundary conditions. Whenever possible also experimental results are mentioned.

In the expansion of a semi-infinite plasma into a vacuum the energetic ion peak propagating supersonically towards the vacuum—as seen in laboratory experiments—is interpreted by means of the Lagrangian fluid description as a relic of a wave breaking scenario of the corresponding inviscid ion dynamics. The inclusion of viscosity is shown numerically to stabilize the associated density collapse giving rise to a well defined fast ion peak reminiscent of adhesive matter.

In purely convection driven flows the Lagrangian flow velocity is given by its initial value and hence the Lagrangian velocity gradient tensor can be evaluated accurately to find out the appearance of singularities in density and vorticity and the emergence of new structures such as wavelets in one-dimension (1D). In cosmology referring to the pancake model of Zel'dovich and the adhesion model of Gurbatov and Saichev, both assuming a clumping of matter at the intersection points of fluid particle trajectories (i.e. at the caustics), the foam-like large-scale structure of our Universe observed recently by Chandra X-ray observatory may be explained by the 3D convection of weakly interacting dark matter.

E-mail address: hans.schamel@uni-bayreuth.de (H. Schamel).
URL: http://www.phy.uni-bayreuth.de/∼btpa20/

0370-1573/$ - see front matter
doi:10.1016/j.physrep.2003.12.002

Recent developments in plasma and nanotechnology—the miniaturization and fabrication of nanoelectronic devices being one example—have reinforced the interest in the quasi-ballistic electron transport in diodes and triodes, a field which turns out to be best treated by the Lagrangian fluid description. It is shown that the well-known space–charge-limited flow given by Child–Langmuir turns out to be incorrect in cases of finite electron injection velocities at the emitting electrode. In that case it is an intrinsic bifurcation scenario which is responsible for current limitation rather than electron reflection at the virtual cathode as intuitively assumed by Langmuir. The inclusion of a Drude friction term in the electron momentum equation can be handled solely by the Lagrangian fluid description. Exploiting the formula in case of field emission it is possible to bridge ballistic and drift-dominated transport. Furthermore, the transient processes in the electron transport triggered by the switching of the anode potential are shown to be perfectly accounted for by means of the Lagrangian fluid description.

Finally, by use of the Lagrangian ion fluid equations in case of a two component, current driven plasma we derive a system of two coupled scalar wave equations which involve the specific volume of ions and electrons, respectively. It has a small amplitude strange soliton solution with unusual scaling properties. In case of charge neutrality the existence of two types of collapses are predicted, one being associated with a density excavation, the other one with a density clumping as in the laser induced ion expansion problem and in the cosmic sticking matter problem. However, only the latter will survive charge separation and hence be observable.

In summary, the Lagrangian method of solving fluid equations turns out to be a powerful tool for compressible media in general. It offers new perspectives and addresses to a broad audience of physicists with interest in fields such as plasma and fluid dynamics, semiconductor- and astrophysics, to mention few of them.

PACS: 05.45.−a; 29.27.Bd; 52.75.Kq; 98.65.−r

Keywords: Lagrangian description; Plasma and gas dynamics; Fast ions; Laser produced plasmas; Density collapses; Cosmic large scale structures; Diode physics; Space–charge-limited currents; Switching of diodes; Current carrying plasmas

Contents

1. Introduction

Structure formation processes in fluids and plasmas, being fundamental issues in modern continuous flow dynamics, have kept their fascination up to the present days. One reason is that many observed phenomena are directly related with the (self-)generation of coherent structures such as density patterns and vortex filaments which in turn may have a profound influence on the global transport e.g. in a confined configuration with prescribed boundary conditions. Another one is the complex nature of the governing equations in space and time which only in rather restricted situations are found to be accessible by analytical methods. Although numerical methods may help to elucidate the involved physics, there is no doubt that a certain observed feature of the dynamics cannot be claimed to be understood completely unless it is accompanied and explained by the corresponding analytical solution.

In cases where a fluid description is available and meaningful, it is usually the Eulerian flow description on which analytical treatments are based. However, there exists another, in a sense complementary description—the Lagrangian fluid description (LFD)—through which the governing equations may be analyzed and solved too. Since such solutions may be easier or sometimes be accessible only by the latter description (see later sections for more details), it seems to be worth to become familiar with this way of analysis, too.

This review reports on recent progress made in the formation of coherent structures by means of LFD. It is to a large extent tutorial and addresses a broad audience of physicists being involved in the pattern formation of dilute, compressible, continuous media comprising areas such as astrophysics, laserphysics, plasma and semiconductor physics.

As it is generally known, the Eulerian description makes use of fields in space–time, such as the density field $n(\boldsymbol{r},t)$ or the velocity field $\boldsymbol{v}(\boldsymbol{r},t)$, whereas in the Lagrangian flow description these quantities are seen and described in a frame moving locally with a fluid element. This in turn implies that each fluid element is distinguishable from the others by a kind of a label such as its position at some fixed time which remains attached to it for all subsequent times.

In the present review four topics are selected which on the one hand show how to proceed and succeed theoretically within the LFD as the common tool but which on the other hand also indicate how new light can be shed by the LFD on the involved physics. These examples are mainly dealing with ionized or neutral compressible gases but can straightforwardly be used for an extension or transformation to ordinary fluids, as well. We shall, if possible, also furnish experimental evidence of the derived results. We aim at four different physical objects for which we want to find an

explanation via the LFD:

- the ion blow-off and the fast ion peak in a laser-produced expanding plasma
- the web of hot gas and dark matter defining the cosmic, intergalactic landscape
- some novel properties of the collective electron transport in plasma and semiconductor diodes
- new dynamical aspects in current driven plasmas.

2. Plasma expansion into vacuum

2.1. Experimental observation

We begin with an experimental observation. A short intense laser pulse focused on a solid target creates almost instantaneously a coronal plasma which starts to expand into the adjacent vacuum. A time-of-flight ion collector placed in front of the target recognizes at sufficiently intense laser intensities high-energy ion current spikes which appear in addition to the ion current stemming from the expanding thermal plasma. A typical measurement (Ehler, 1975) made by a high-power CO_2 laser pulse on a flat polyethylene target, is shown in Fig. 1. It shows the ion current signal vs time for various target irradiances Φ. If $\Phi \sim 10^{12}$ W/cm^2 (a) a photoelectron pulse is seen at $t = 0$, which marks the onset of the ns laser pulse, followed by the broad plasma signal. At higher laser irradiances with a threshold of about 5×10^{12} W/cm^2 in addition high-energy ion peaks preceding the thermal plasma pulse are seen on the ion current trace (b)–(d). Obviously, ions of different charge and mass were accelerated during the expansion process reaching energies of about 100 keV and higher (at $\Phi \sim 2 \times 10^{14}$ W/cm^2 the H^+ ion energy was 140 keV). Here, an expanding multi ion species plasma had been investigated. If instead, the laser would have been irradiated on a frozen hydrogen (or deuterium) target only the energetic H^+ (or D^+) peak would remain.

Two questions arise from these observations:

(i) what causes the ions to reach such high supersonic velocities?
(ii) how is the peak coming from?

An answer will be given in the next paragraphs of this section.

2.2. Modeling of plasma expansion

Our ultimate goal is to understand the dynamical evolution of the expanding plasma after the moment of its creation by the laser pulse. Following Sack and Schamel (1987), we assume a two component plasma consisting of one ion species and electrons and describe it by an electrostatic two-fluid approach:

$$\partial_t n_s + \nabla \cdot (n_s \boldsymbol{v}_s) = 0 \ ,$$

$$m_s[\partial_t + \boldsymbol{v}_s \cdot \nabla]\boldsymbol{v}_s = -q_s \nabla\phi - \frac{1}{n_s}\nabla p_s, \quad s = e, i \ ,$$

$$\nabla^2\phi = \frac{e}{\varepsilon_0}(n_e - n_i)$$

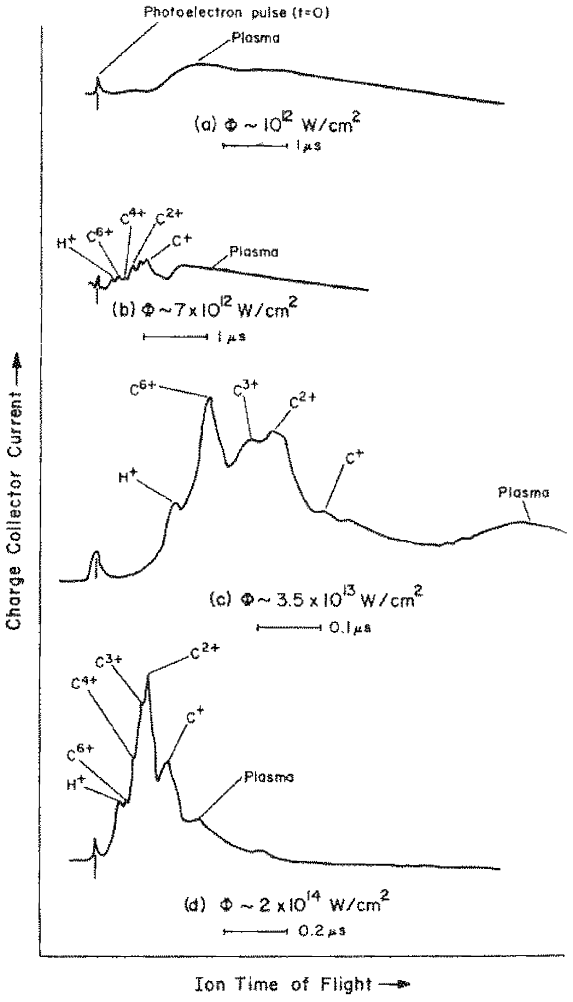

Fig. 1. Examples of single-shot ion current signal vs time for various target (polyethylene) irradiances Φ (from Ehler, 1975).

which represent continuity and momentum equation for each species, assuming single charged ions ($-q_e = q_i = e$). The third equation is Poisson's equation (or Gauss' law). We further assume that the process is planar, i.e. one-dimensional (1D) in space ($\nabla \to \hat{x}\partial_x$), and that the evolution takes place on the ionic time scale such that the electrons are in a quasi equilibrium state represented (for simplicity) by an isothermal pressure law, $p_e \sim n_e$. (We note that in Sack and Schamel (1987) also an adiabatic pressure law, $p_e \sim n_e^\gamma$, was treated with γ, the adiabatic exponent.) The ion pressure p_i will be neglected further on. This is in accord with the observation that at least at high laser intensities the absorbed energy goes primarily into the electrons. The ions are assumed to occupy initially the half space, $x < 0$, with a steep, step-like front at $x=0$ (the so-called diaphragm problem).

In the unperturbed, quasi-neutral plasma ($x \to -\infty$), we have equal densities $n_e = n_i = n_0$, zero velocity and a constant electron temperature T_{e0}, such that $p_{e0} = n_0 k T_{e0}$, where k is the Boltzmann

constant. Normalizing the densities by n_0, the electric potential by $kT_{e0}e^{-1}$, the coordinate by the Debye length $\lambda_D \equiv \sqrt{\varepsilon_0 kT_{e0}/n_0 e^2}$, the time by the inverse ion plasma frequency $\omega_{p_i}^{-1} \equiv \sqrt{\varepsilon_0 m_i/n_0 e^2}$ and the ion velocity by the ion acoustic velocity $c_s = \sqrt{kT_{e0}/m_i} \equiv \lambda_D \omega_{p_i}$, we arrive at the following system of coupled equations:

$$\partial_t n + \partial_x(nv) = 0 \ , \tag{1a}$$

$$\partial_t v + v\partial_x v = -\partial_x \phi = E \ , \tag{1b}$$

$$\partial_x^2 \phi = n_e(\phi) - n \ , \tag{1c}$$

where E is the electric field and $n_e(\phi)$ is given by the Boltzmann law

$$n_e(\phi) = \exp \phi \tag{2}$$

which follows by integration of the electron momentum equation in the limit of inertia less electrons ($m_e \to 0$). System (1), (2) has to satisfy the boundary conditions at $x \to -\infty$ (unperturbed, resting, neutral plasma) and at $x \to +\infty$ (vacuum conditions):

$$\begin{aligned} &n(x \to -\infty, t) = 1 \ , \\ &n(x \to +\infty, t) = 0, \quad \phi(x \to -\infty, t) = 0 \ , \\ &v(x \to \pm\infty, t) = 0, \quad \phi(x \to +\infty, t) \to -\infty \ . \end{aligned} \tag{3}$$

The latter condition stems from the vacuum condition $n_e \to 0$ as $x \to +\infty$. In addition, the system is subject to the initial conditions

$$n(x,0) = n^0(x), \quad v(x,0) = 0, \quad \phi(x,0) = \phi^0(x) \ . \tag{4}$$

In (4) $n^0(x)$ is prescribed and assumed to be step-like, and $\phi^0(x)$ follows self-consistently from the nonlinear Poisson equation

$$\partial_x^2 \phi^0(x) = e^{\phi^0(x)} - n^0(x) \ . \tag{5}$$

There is, hence, already at $t=0$ an electric field $E^0(x) = -\phi^{0\prime}(x)$ which results from charge separation and which will accelerate the ions, since a decreasing potential implies a positive field.

At present, even this simple system (1)–(5) is too complicated to be treated entirely by analytical methods. We, hence, have to refer to a numerical solution, to learn more about its dynamical properties. If they are known we then can draw further conclusions.

This step is, however, nontrivial as typical codes, based on a discretization of the Euler system (1), cannot elaborate the desired features. The reason is that these codes are diffusive and dispersive and are hence in conflict with the collisionless, ideal nature of the fluid. We have to invoke a Lagrangian code to keep this property during the evolution.

2.3. Lagrangian fluid description and code

As said before, the LFD makes use of the concept of a fluid element the trajectory of which is described in time τ by the quantity $x(x_0, \tau)$. At $\tau = 0$ the fluid element is located at x_0, $x(x_0, 0) = x_0$,

and at time τ it is at the Euler position x. Its velocity is assumed to coincide with the actual fluid velocity at its actual position:

$$\dot{x}(x_0,\tau) = v(x(x_0,\tau),\tau) \equiv \tilde{v}(x_0,\tau)\ . \tag{6}$$

Dot (and later dash) means differentiation with respect to $\tau(x_0)$ at fixed $x_0(\tau)$. In the second equality sign we have introduced the velocity in the Lagrangian frame of coordinates x_0,τ, denoted by tilde, and we have made use of an identity relating the Eulerian quantity $v(x,t)$ with the Lagrangian one $\tilde{v}(x_0,\tau)$. Integrating (6) with respect to τ at fixed x_0 we arrive at

$$\begin{aligned} x(x_0,\tau) &= x_0 + \int_0^\tau \mathrm{d}t'\tilde{v}(x_0,t')\ , \\ t(x_0,\tau) &= \tau \end{aligned} \tag{7}$$

which provides a coordinate transformation from Lagrangian (x_0,τ) to Eulerian (x,t) coordinates. The Jacobian of this transformation is given by

$$J(x_0,\tau) := x'(x_0,\tau) = 1 + \int_0^\tau \mathrm{d}t'\tilde{v}'(x_0,t') \tag{8}$$

from which follows immediately that

$$\dot{J}(x_0,\tau) = \tilde{v}'(x_0,\tau) \tag{9}$$

and that at a given time $\tau = t$ the volume element in 1D or the distance between two neighboring trajectories $\mathrm{d}x := x(x_0+\mathrm{d}x_0,t) - x(x_0,t)$ is in lowest nontrivial order given by

$$\mathrm{d}x = J(x_0,t)\,\mathrm{d}x_0\ . \tag{10}$$

This is shown in Fig. 2, where two trajectories are plotted, which may intersect at $\tau = t_*$ (see later).

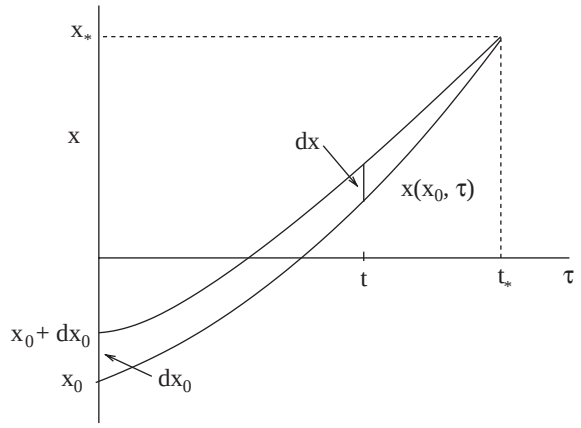

Fig. 2. Two intersecting trajectories as functions of time.

The relationship between Eulerian and Lagrangian derivatives follows from (6)–(8) and becomes

$$\partial_{x_0} = x'(x_0,\tau)\partial_x + t'(x_0,\tau)\partial_t = J(x_0,\tau)\partial_x \ , \tag{11a}$$

$$\partial_\tau = \dot{x}(x_0,\tau)\partial_x + \dot{t}(x_0,\tau)\partial_t = \tilde{v}(x_0,\tau)\partial_x + \partial_t = \partial_t + v\partial_x \ , \tag{11b}$$

where in the last step again the identity $\tilde{v}(x_0,\tau) \equiv v(x,t)$ was used.

Uniqueness of this transformation requires non-vanishing J or from (8)

$$\int_0^\tau \mathrm{d}t'\tilde{v}'(x_0,t') \neq -1 \ . \tag{12}$$

If it happens that the positive J approaches zero, say at $\tau = t_*$, the Eulerian derivative ∂_x in (11a) becomes singular and the volume element $\mathrm{d}x$ in (10) shrinks to zero, Fig. 2.

It then follows that the continuity equation (1a) can be decomposed and transformed as

$$(\partial_t + v\partial_x)n + n\partial_x v \equiv \partial_\tau \tilde{n} + \tilde{n}\frac{1}{J}\tilde{v}' = 0 \ .$$

Replacing $\tilde{v}'(x_0,\tau)$ by $\dot{J}(x_0,\tau)$ because of (9) we can write the last equation as $\partial_\tau ln(\tilde{n}J) = 0$ and get for the Lagrangian density by integration

$$\tilde{n}(x_0,\tau) = \frac{n^0(x_0)}{J(x_0,\tau)} \ , \tag{13}$$

where $n^0(x_0)$ is a constant with respect to τ, representing the initial density distribution. The ion motion is hence governed in Lagrange space by

$$\dot{x}(x_0,\tau) = \tilde{v}(x_0,\tau) \ , \tag{14a}$$

$$\dot{\tilde{v}}(x_0,\tau) = \tilde{E}(x_0,\tau) \equiv E(x(x_0,\tau),\tau) \ , \tag{14b}$$

$$\tilde{n}(x_0,\tau)J(x_0,\tau) = n^0(x_0) \tag{14c}$$

and by Poisson's equation. The initial conditions are $\tilde{n}(x_0,0) = n^0(x_0)$ and $x(x_0,0) = x_0$.

Introducing a discretized mesh in space x_0 and time τ, one can easily advance the system in time finding the trajectories at each new time step if their position is known at the previous one [for more details see e.g. Appendix C of Sack and Schamel (1987)]. In the discretized version $J(x_0,\tau)$ is replaced by the finite difference approximation of (10), namely $J(x_0,\tau) \simeq \Delta(x_0,\tau)/\Delta x_0$ where $\Delta(x_0,\tau)$ measures the finite size width of the fluid element at τ. Note that Poisson's equation is nonlinear and can be solved iteratively at each instant τ [see Section 4 and Appendix B of Sack and Schamel (1987)].

The advantage of such a Lagrangian scheme is the absence of a convective term $v\partial_x v$, which causes most trouble in Eulerian schemes, as well as the absence of numerical dissipation and dispersion, which usually lead to an undesirable strong smoothing of the solution. In the Lagrangian scheme, the difference mesh is coupled to the local flow velocity, so that a strong inhomogeneity in the velocity and in the density profile are resolved in an optimum manner.

Let us, before presenting the numerical results of our plasma expansion problem, add a remark which refers to a different Lagrangian variable, the "mass" variable η. Making use of (10) and (14c) we can define $\eta(x,t) \equiv \tilde{\eta}(x_0,\tau)$ as

$$\eta(x,t) := \int_0^x n(x',t)\,\mathrm{d}x' = \int_0^{x_0} n^0(\xi)\,\mathrm{d}\xi \equiv \tilde{\eta}(x_0,\tau)\ . \tag{15}$$

It immediately follows using (11b) and the last equation of (15) that

$$(\partial_t + v\partial_x)\eta(x,t) \equiv \hat{\partial}_\tau \tilde{\eta}(x_0,\tau) = 0 \tag{16}$$

which implies that η is constant along the trajectory being hence a stream function which can be used as a Lagrangian variable (label). For the Eulerian derivatives we then have from (15) and (16)

$$\partial_x \eta(x,t) = n(x,t)\ , \tag{17a}$$

$$\partial_t \eta(x,t) = -n(x,t)v(x,t) \tag{17b}$$

from which the validity of mass conservation is directly seen, since of course $\partial_t\partial_x\eta = \partial_x\partial_t\eta$.

2.4. Numerical solution of inviscid ion expansion—wave breaking

Making use of the Lagrangian code described in Section 2.3, we obtain the following numerical results for our system (1)–(5) shown in Fig. 3. Fig. 3a shows the initial step-like ion density and the initial electric field as functions of x as Eulerian quantities. The electric field—also called ambipolar electric field—is non-monotonic and arises from charge separation, Eq. (1c), which is due to the high (in our case, infinite) electron mobility. Electrons already at $t = 0$ occupy the full space (not shown in Fig. 3) with a much less steep density gradient than that of the ions.

Fig. 3b shows for a later time $t = 17$ ion density and velocity as functions of space as well as the ambipolar electric field. The density profile has become less steep and has acquired a peak or a cusp-like ion front at $x \approx 0$. (Note that at $t = 0$ the ion front was located around $x = -40$.) The ion velocity, which was initially zero, is non-monotonic and positive, having a large negative slope at the ion front. Ion acceleration maximizes at this point, as seen by the strongly peaked electric field at $x \approx 0$. Fig. 3c shows on an enlarged scale the evolution of the ion front from $t = 13$ up to $t = 17$. We see that rather suddenly a strong peak emerges at the ion front. It turns out that this peak further narrows and becomes infinite at $x_* = 4.11, t_* = 17.94$ i.e. the ion front becomes singular at these coordinates.

The explanation is rather simple. What happens is the first intersection of two trajectories, as indicated already in Fig. 1. Since this collapsing fluid element behaves according to (10) and (13) as $n\,\mathrm{d}x = n^0\,\mathrm{d}x_0 \neq 0$ the vanishing of its width $\mathrm{d}x$ is accompanied by a singularity in n. In Euler space we get near the singular point for $t \to t_*$ (see Section 2.5):

$$n \sim \frac{1}{t_* - t}\ , \tag{18a}$$

$$v \sim \frac{x_* - x}{t_* - t} \tag{18b}$$

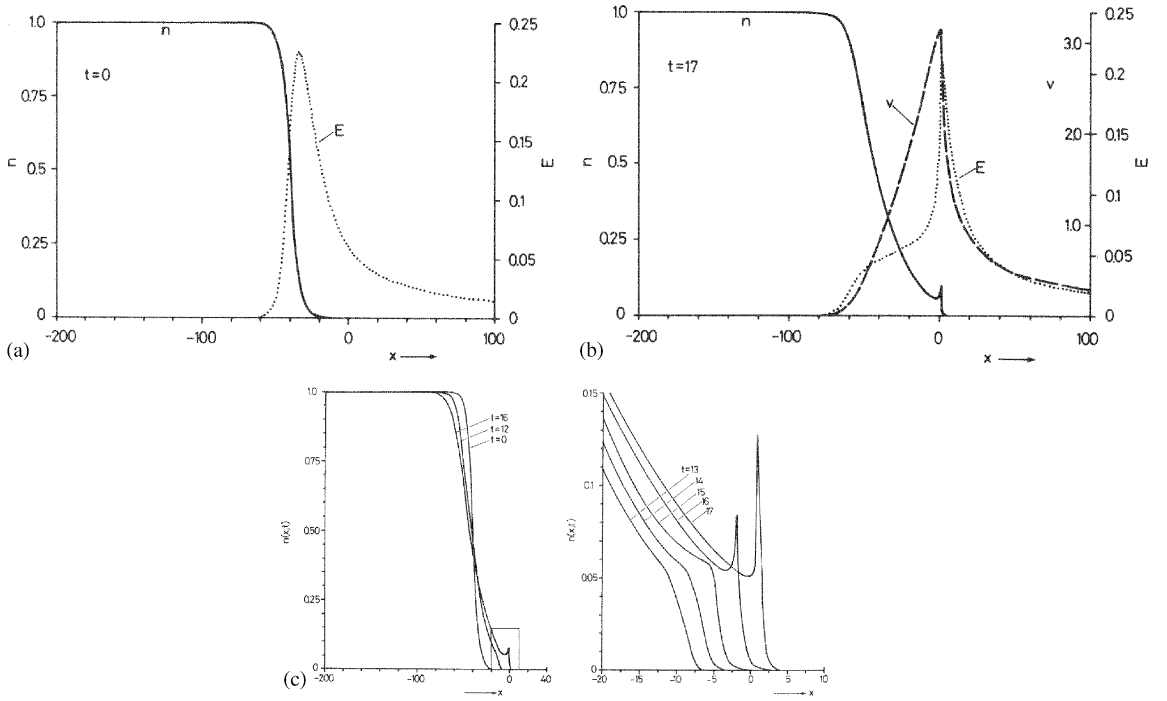

Fig. 3. (a) Initial ion density and electric field as functions of x. (b) Ion density, electric field and ion velocity as functions of x at $t=17$. (c) Ion density as a function of x at different times; the second part shows the density front on an enlarged scale (from Sack and Schamel, 1987).

which satisfy

$$\partial_t n + \partial_x(nv) = 0 \ , \tag{19a}$$

$$\partial_t v + v\partial_x v = 0 \ . \tag{19b}$$

At the front a wave steepening and ion bunching process takes place, described by the simple wave equation (19b), the velocity gradient is becoming singular, $-\partial_x v \to \infty$, for $x \to x_*, t \to t_*$.

Hence, the inviscid ion expansion undergoes a wave collapse beyond which the hydrodynamic description breaks down.

We mention that in this last stage the electric potential behaves like $\phi \sim -\ln(t_* - t)$ from which follows that the electric field disappears. The collapsing fluid element in the final stage no longer experiences a force and is hence simply determined (driven) by convection.

Let us prove (18a) in a separate section before we continue to describe the plasma expansion in the post collapse phase.

2.5. The scalar wave equation

We first show that our system in Lagrangian space can be described by a single second order wave equation. For this purpose we change to the mass variable as a Lagrangian coordinate and

introduce the specific volume $V(\eta,\tau) := 1/n(\eta,\tau)$, where, for simplicity, we use the same symbol for the Lagrangian dependent quantities and suppress tilde. Note that $V(\eta,\tau)$ is nothing else but the Jacobian formulated in terms of the new mass variable since it holds via (15) $\mathrm{d}x = V(\eta,\tau)\,\mathrm{d}\eta$. We then have with $\partial_x = (1/V)\partial_\eta$ which follows from (11a), (13) and (15),

$$\dot{x}(\eta,\tau) = v(\eta,\tau)\ , \tag{20a}$$

$$\dot{v}(\eta,\tau) = E(\eta,\tau) = -\frac{1}{V(\eta,\tau)}\phi'(\eta,\tau)\ , \tag{20b}$$

$$x'(\eta,\tau) = V(\eta,\tau)\ , \tag{20c}$$

where dash refers to ∂_η. Poisson's equation becomes after a multiplication with V

$$\left[\frac{1}{V}\,\phi'(\eta,\tau)\right]' = V(\eta,\tau)n_e(\phi(\eta,\tau)) - 1\ . \tag{21}$$

From this follows, using Eq. (20), that

$$\ddot{V} = \dot{x}' = \dot{v}' = -\left[\frac{1}{V}\,\phi'\right]'\ . \tag{22}$$

Combining (21) with (22) we get

$$n_e(\phi) = \frac{1-\ddot{V}}{V} \equiv e^{\phi}$$

so that $\phi(\eta,\tau) = \ln((1-\ddot{V})/V)$. Inserting this expression finally into (22) (and returning to the differential symbol ∂_η) we get (Sack and Schamel, 1987):

$$\ddot{V} + \partial_\eta\left[\frac{1}{1-\ddot{V}}\,\partial_\eta\left(\frac{1-\ddot{V}}{V}\right)\right] = 0\ . \tag{23}$$

Hence, in the Lagrange space (η,τ) the Eulerian coupled system (1), (2) is fully governed by the single scalar wave equation (23), which is an equation for the Jacobian.

This equation is nonlinear and still too complicated to be solved for our given initial value problem. This means that we are still not in the position to predict the singular data x_*, t_* for given initial conditions. We, however, can easily get a trivial partial solution

$$V(\eta,\tau) = a(t_* - \tau)[1 + \cdots]\ , \tag{24}$$

where $0 < t_* - \tau \ll 1$, a is a constant and higher order terms have already been neglected. Eq. (24) corresponds to (18a) and describes the collapsing fluid element. Therefore, the system admits a singular solution, and we know from our Lagrangian numerical investigation that for a sufficiently steep initial ion density profile this singular solution (24) is indeed adopted by a specific fluid element. For more details of V and the other quantities we refer to Sack and Schamel (1987).

For t exceeding t_* we have two options. Either we stay in the collisionless regime in which case multistreaming and the transition to a kinetic Vlasov description would be necessary, or we allow for some weak collisions, in which case the ideal Euler-like equation (1b) may be replaced by the dissipative Navier–Stokes-like equation. In the latter case, we are able to follow the plasma expansion into vacuum numerically for longer times.

2.6. Numerical solution of viscid plasma expansion—fast ion peak

We include in the ion momentum equation a viscous term such that (1b) is replaced by

$$\partial_t v + v\partial_x v = -\partial_x \phi + v\partial_x^2 v \tag{25}$$

and transit to Lagrange space (x_0, τ). The corresponding viscous term, added to (14b), is expected to smooth to some extent the ion peak. What we find numerically is shown in Fig. 4a, which shows for the same initial conditions the space–time evolution of the ion density in Eulerian space. We again recognize an ion bunching process which takes place near $t_* \approx 18$. This time, however, the cusp-like ion peak stabilizes and remains dominant until $t_0 \approx 100$, maximizing at $t_M = 95$. Later it strongly diminishes although it remains existent for all later times. From Fig. 4b which shows n, v and E at 3 times steps around the time t_M of maximum bunching, we learn that a debunching process takes place after t_M. At $t_M = 95$ the velocity maximum overtakes the ion peak and hence $\partial_x v$ changes sign and debunching sets in. Due to mass conservation, $n\Delta = \text{const.}$, an increase of Δ causes a decrease of n. Therefore, it is not dissipation which causes the sudden decrease of the density peak, but debunching.

Fig. 4c shows the time evolution of the maximum electric field $E_{\max}$ and of the velocity v_f of the ion peak (front) for three values of ν. For $t > t_M$ the maximum electric field decreases as a result of debunching, and the ion peak velocity still increases. Although E goes down, the curvature of v at the front decreases as well, such that v_f continues to become larger. For isothermal electrons, $p_e \sim n_e^\gamma$ with $\gamma = 1$, v_f increases without bounds. For $1 < \gamma < 2$, corresponding to some electron cooling during expansion, we mention that there is an upper limit given by the self-similar expression $v_f^{ss}(\gamma) = 2\sqrt{\gamma}/(\gamma - 1)$ (for more details, see Sack and Schamel, 1987).

The physics involved in the laser produced plasma expansion may include further effects such as supra-thermal electrons, non-planar effects, ponderomotive field effects etc. However, its basic features, being extracted by the Lagrangian flow description, can be summarized as follows:

- the ion blow-off (and with it the existence of fast ions) is a result of the ambipolar electric field which establishes and which accelerates the ions to supersonic velocities
- a definite ion front (peak) remains for all times being a relic of the ideal wave breaking or unlimited ion bunching process.

We also have learned that near collapse the ideal ion fluid in 1D is simply convection driven, as the inertia terms in the momentum equation dominate over the electric force term.

The existence of such regimes has motivated us to consider forceless fluid (plasma) motions also in higher dimensions.

3. Purely convection driven structures in higher dimensions

In this section we are interested in non- or weakly interacting fluids such as a dilute cold gas. That means we keep only the inertia terms in the momentum equation but take into account more seriously the initial conditions. Our goal is to learn more about the appearances of singularities or caustics and to apply the knowledge to pattern formation in the Universe.

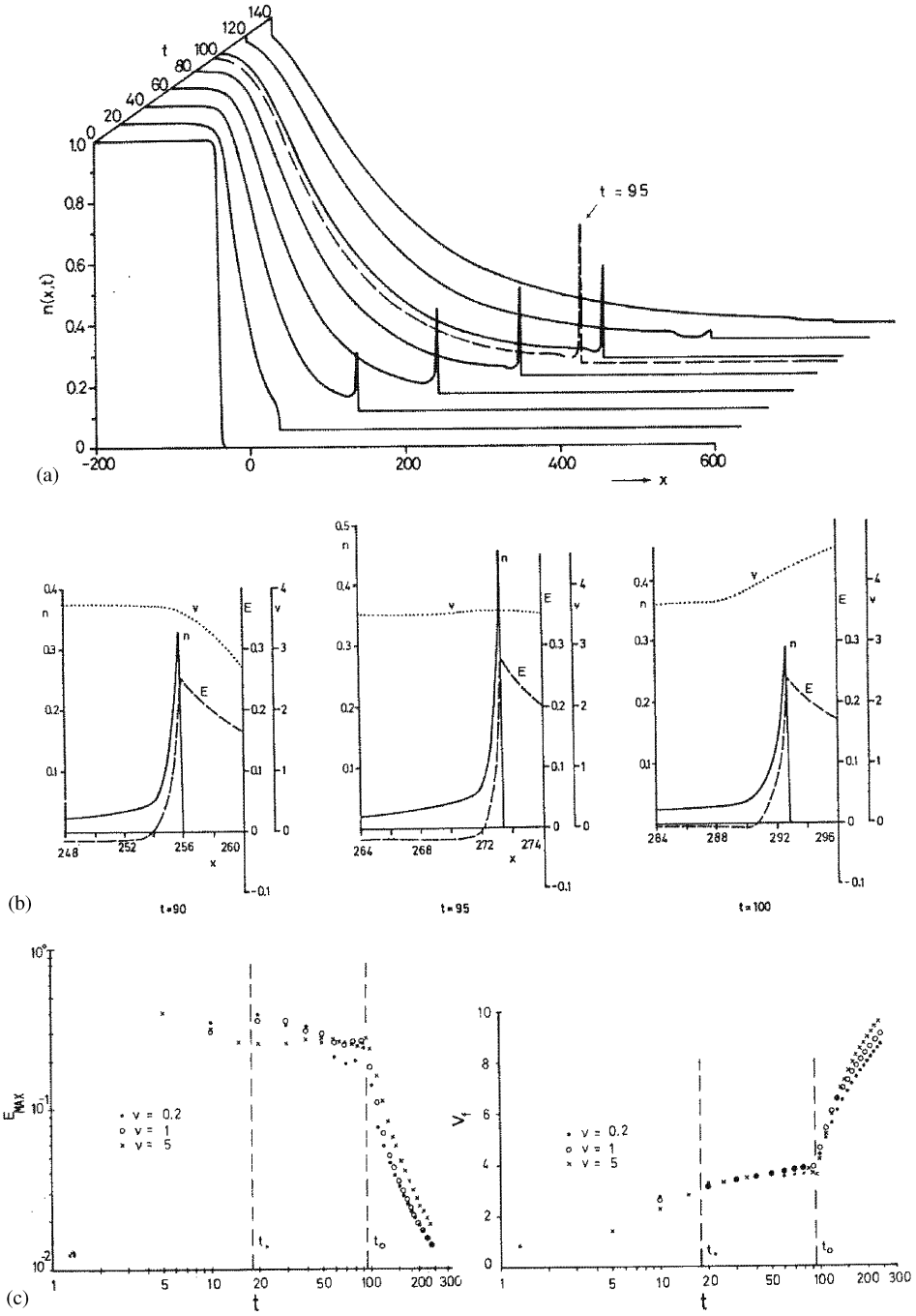

Fig. 4. (a) Space–time evolution of the ion density for $v = 5$ in the interval $0 \leqslant t \leqslant 140$, at $t = 95$ (dashed curve) ion bunching maximizes whereas for $t > 95$ debunching takes place. (b) Spatial dependence of ion density n, velocity v and electric field E at three different times around maximum ion bunching. $t = t_M = 95$ the velocity maximum overtakes the density peak causing debunching. (c) Time dependence of maximum electric field (left) and of ion front velocity (right) on a logarithmic time scale ($t_0 \equiv t_M$) (from Sack and Schamel, 1987).

We start for an introduction with the simplest situation, namely that of a 1D purely convection driven fluid.

3.1. Density collapse and the emergence of new density structures in 1D

Our forceless, compressional gas is hence governed in Eulerian space by

$$\partial_t n + \partial_x(nv) = 0 \ , \tag{26a}$$

$$\partial_t v + v\partial_x v = 0 \tag{26b}$$

subject to the initial conditions

$$n(x,0) = n_0(x) \ , \tag{27a}$$

$$v(x,0) = v_0(x) \ . \tag{27b}$$

In the Lagrangian space (x_0,τ), referring to Section 2.3, the system becomes

$$\tilde{n}(x_0,\tau) = \frac{n_0(x_0)}{J(x_0,\tau)} \ , \tag{28a}$$

$$\partial_\tau \tilde{v}(x_0,\tau) = 0 \ . \tag{28b}$$

The last equation is easily solved:

$$\tilde{v}(x_0,\tau) = v_0(x_0) \tag{29}$$

and with it, the Jacobian (8) is completely known

$$J(x_0,\tau) = 1 + \int_0^\tau \mathrm{d}t' v_0'(x_0) = 1 + \tau v_0'(x_0) \tag{30}$$

such that, if the inversion to Euler space can be accomplished, everything is known. Following Karimov and Schamel (2001) we ask for the occurrence of singularities and the emergence of new density structures.

(i) singularities

A singularity in $\tilde{n}$ (or n) occurs when $J(x_0,\tau)$ vanishes for the first time according to (28a), which requires via (30) an interval I in the $v_0(x_0)$ profile in which v_0 is decreasing:

$$J(x_{0*},\tau_*) = 0, \quad \tau_* = \min_{x_0\in I}\left[\frac{-1}{v_0'(x_0)}\right] \equiv \frac{-1}{v_0'(x_{0*})} > 0 \ . \tag{31}$$

Or said in different words, two trajectories [or characteristics of (26b)] which start near the position of maximum negative slope of $v_0(x_0)$: $x_{0*} + \mathrm{d}x_0$ and x_{0*}, respectively, will intersect first namely at τ_*. In the present case, the trajectories are known, being straight lines:

$$x(x_0,\tau) = x_0 + \tau v_0(x_0) \tag{32}$$

and it holds to lowest order in the differentials for fixed τ

$$\mathrm{d}x := x(x_0 + \mathrm{d}x_0,\tau) - x(x_0,\tau) \simeq [1 + \tau v_0'(x_0)]\,\mathrm{d}x_0 \tag{33}$$

which vanishes first for (31).

(ii) new extrema

From (11a) we know that

$$\partial_x n(x,t) = \frac{1}{J(x_0,\tau)}\partial_{x_0}\tilde{n}(x_0,\tau) \tag{34}$$

and hence a new extremum arises when $\partial_{x_0}\tilde{n}(x_0,\tau)$ becomes zero for the first time for a non-vanishing Jacobian. Making use of (28a) and defining:

$$\theta_0(x_0) := \frac{n_0(x_0)}{n_0'(x_0)}v_0''(x_0) - v_0'(x_0)\ , \tag{35a}$$

$$T(x_0,\tau) := \frac{1}{\tau} - \theta_0(x_0) \tag{35b}$$

we get

$$\partial_{x_0}\tilde{n}(x_0,\tau) = \frac{n_0'(x_0)\tau}{J^2}T(x_0,\tau) \tag{36}$$

and hence the roots of $T(x_0,\tau)$ determine the extremal points (x_{0m},τ_m):

$$T(x_{0m},\tau_m) = 0\ . \tag{37}$$

Let us illustrate this by two examples (Karimov and Schamel, 2001), starting initially from a Gaussian density profile: $n_0(x_0) = \exp(-x_0^2/2)$.

In the first case, we take $v_0(x_0) = x_0\exp(-x_0)$, $x_0 > 0$, which is a single humped velocity profile. Fig. 5a shows the evolution of the Eulerian density in space and time with the emergence of a new propagating maximum and its collapse at x_*, t_*.

In the second case, we take $v_0(x_0) = x_0 + B\sin kx_0$, $x_0 > 0$, where an oscillatory initial velocity perturbation is superimposed on the linear profile. One can show (Karimov and Schamel, 2001), that a simultaneous multiple collapse arises when $kB > 1$, in which case regions of negative slopes of $v_0(x_0)$ occur periodically in space.

On the other hand, when $kB < 1$, the function $\theta_0(\xi)$ in (35a) has qualitatively a shape shown in Fig. 5b. When it is cut by $1/\tau$ we know from (35b) that $T(x_0,\tau)$ and from (36) that $\partial_{x_0}\tilde{n}(x_0,\tau)$ vanish corresponding to an extremum. Fig. 5c shows qualitatively the Eulerian space–time evolution of $n(x,t)$. Initially, there is only one maximum. At a later time τ_1 the cut of $1/\tau_1$ with $\theta_0(\xi)$ has 2 solutions corresponding to a new pair of extrema, a minimum and a maximum. For τ_2 the cut exhibits 4 solutions and hence a second new pair arises, and so on. We hence get a wavelet structure on the initially monotonic density profile driven by the initial velocity $v_0(x_0)$. In case of $kB > 1$ an emerging hump of the wavelet structure can itself be subject to collapse such that a rich spatial-temporal pattern may arise, depending on the parameters k and B.

We learn that a variety of structures can emerge already in 1D driven by convection.

3.2. Density and vorticity collapse in 2D and 3D

In 2D and 3D a new quality comes into play namely the vorticity $\boldsymbol{\omega} = \nabla\times\boldsymbol{v}$, assuming, in generality, a non-potential flow. Considering the initial value problem (Schamel and Karimov, 2000;

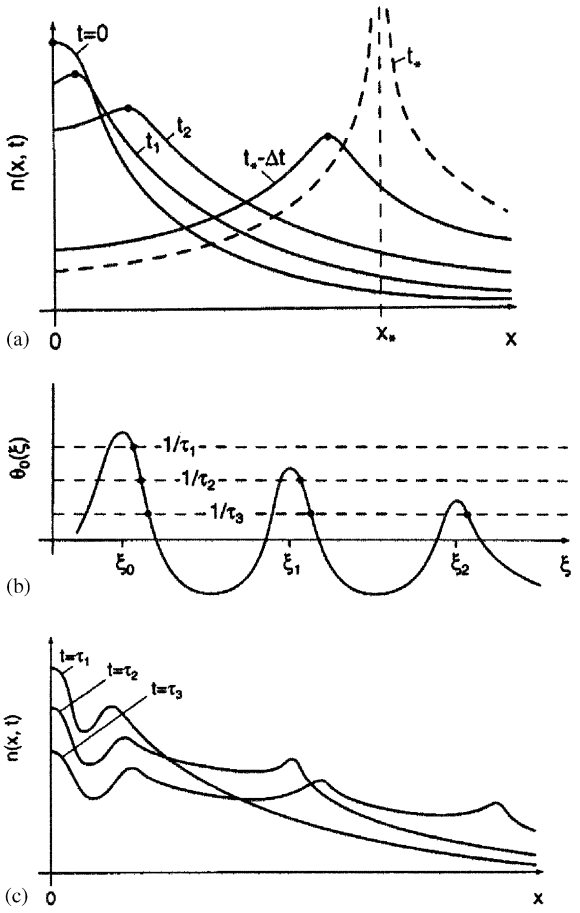

Fig. 5. (a) Qualitative density behavior in space and time. The emerging maximum collapses at $x = x_*$ and $t = t_*$. (b) The qualitative behavior of $\Theta_0(\xi)$. (c) The space–time evolution of the density with the appearance of a wavelet structure (from Karimov and Schamel, 2001).

Karimov and Schamel, 2002)

$$\partial_t n + \nabla \cdot (n\boldsymbol{v}) = 0 \ , \tag{38a}$$

$$\partial_t \boldsymbol{v} + \boldsymbol{v} \cdot \nabla \boldsymbol{v} = 0 \tag{38b}$$

with

$$n(\boldsymbol{r}, 0) = n_0(\boldsymbol{r}) \ , \tag{39a}$$

$$\boldsymbol{v}(\boldsymbol{r}, 0) = \boldsymbol{v}_0(\boldsymbol{r}) \tag{39b}$$

we get in Lagrange space from (38b)

$$\partial_\tau \tilde{\boldsymbol{v}}(\boldsymbol{r}_0, \tau) = 0$$

which has the solution

$$\tilde{\boldsymbol{v}}(\boldsymbol{r}_0,\tau)=\boldsymbol{v}_0(\boldsymbol{r}_0)\ . \tag{40}$$

The trajectory of a fluid element is then found to be

$$\boldsymbol{r}(\boldsymbol{r}_0,\tau)=\boldsymbol{r}_0+\tau\boldsymbol{v}_0(\boldsymbol{r}_0) \tag{41}$$

and the relationship between the two different sets of gradients is given by

$$\nabla_0=\underline{\underline{A}}\cdot\nabla \tag{42}$$

with

$$\underline{\underline{A}}=\underline{\underline{I}}+\tau\cdot\underline{\underline{W}}\ , \tag{43}$$

where $\underline{\underline{I}}$ is the unit tensor in $\mathbb{R}^2$ or $\mathbb{R}^3$ and $\underline{\underline{W}}$ refers to the Lagrangian velocity gradient tensor

$$\underline{\underline{W}}=\nabla_0\boldsymbol{v}_0\ . \tag{44}$$

The Jacobian, being the determinant of $\underline{\underline{A}}$, is found to be

$$J(\boldsymbol{r}_0,\tau)=\begin{cases}1+s_0\tau+d_0\tau^2, & \text{2D}\ ,\\ 1+s_0\tau+d_0\tau^2+p_0\tau^3, & \text{3D}\ ,\end{cases} \tag{45}$$

where

$$s_0=\nabla_0\cdot\boldsymbol{v}_0=Sp(\underline{\underline{W}})\ , \tag{46a}$$

$$d_0=\frac{1}{2}[s_0^2-Sp(\underline{\underline{W}}^2)]\ , \tag{46b}$$

$$p_0=\det\underline{\underline{W}} \tag{46c}$$

which are general invariants of the tensor $\underline{\underline{W}}$. $Sp(\underline{\underline{W}})$ refers to Spur (or trace) of the tensor $\underline{\underline{W}}$. So, it is clear that the coefficients of (45) do not depend on the coordinate system and may be calculated in that system where the tensor $\underline{\underline{W}}$ has its simplest form. We then get for density and vorticity (Schamel and Karimov, 2000; Karimov and Schamel, 2002)

$$\tilde{n}(\boldsymbol{r}_0,\tau)=\frac{n_0(\boldsymbol{r}_0)}{J(\boldsymbol{r}_0,\tau)}\ , \tag{47a}$$

$$\tilde{\boldsymbol{\omega}}(\boldsymbol{r}_0,\tau)=\frac{1}{J(\boldsymbol{r}_0,\tau)}\begin{cases}\omega_0\hat{z}, & \text{2D}\ ,\\ \boldsymbol{\omega}_0\cdot[\underline{\underline{I}}+\tau\underline{\underline{W}}], & \text{3D}\ ,\end{cases} \tag{47b}$$

where use was made of $\tilde{\boldsymbol{\omega}}(\boldsymbol{r}_0,0)=\boldsymbol{\omega}_0=\nabla_0\times\boldsymbol{v}_0(\boldsymbol{r}_0)$. The key element is again played by the Jacobian J in the denominator of (47). As in the previous paragraph we can search for new local extrema in $\tilde{n}$ and $\tilde{\boldsymbol{\omega}}$, and by investigating the roots of $J=0$ we can predict the emergence of singularities in the flow. We mention that the nominator of $\tilde{\boldsymbol{\omega}}$ in 3D is still depending on τ which is a relic of vortex stretching that is absent in 2D. The latter is seen by an application of Cauchy's formula

(Lamb, 1932) which expresses the fact that vortex lines are material lines.

$$\tilde{\boldsymbol{\omega}}/\tilde{n} = \left(\frac{\boldsymbol{\omega}_0}{n_0}\cdot\nabla_0\right)\boldsymbol{r}(\boldsymbol{r}_0,\tau)\ . \tag{48}$$

Taking the time derivative of (48) we get using (40), (41)

$$\partial_\tau(\tilde{\boldsymbol{\omega}}/\tilde{n}) = \left(\frac{\boldsymbol{\omega}_0}{n_0}\cdot\nabla_0\right)\tilde{\boldsymbol{v}}(\boldsymbol{r}_0,\tau) = \frac{\boldsymbol{\omega}_0}{n_0}\cdot\nabla_0\boldsymbol{v}_0 = \frac{\boldsymbol{\omega}_0}{n_0}\cdot\underline{\underline{W}} \tag{49}$$

which is solved by (47b) with the initial condition given by (39). Note that (49) in Eulerian space becomes the well-known Beltrami–Helmholtz equation

$$\frac{\mathrm{d}}{\mathrm{d}t}(\boldsymbol{\omega}/n) = \left(\frac{\boldsymbol{\omega}}{n}\cdot\nabla\right)\boldsymbol{v}\ , \tag{50}$$

where $\mathrm{d}/\mathrm{d}t$ is the total or convective time derivative. The righthand side of (50) represents the directional spatial derivative of $\boldsymbol{v}$ along the direction of the vorticity, being termed vortex stretching of the straining flow.

The constancy of $\boldsymbol{\omega}/n$—the Ertel theorem—requires the absence of vortex stretching which in Lagrangian space through (49) becomes $\underline{\underline{W}}\cdot\boldsymbol{\omega}_0 = 0$. The latter has nontrivial solutions $\boldsymbol{\omega}_0$ only if $p_0 = \det\underline{\underline{W}} = 0$ in which case the 3D flow becomes quasi 2D as far as J in (45) is concerned.

One way of getting finite time singularities in the flow driven by advection is to investigate the eigenvalues and eigenvectors of the velocity gradient tensor $\nabla\boldsymbol{v}(\boldsymbol{r},t)$, to see in which direction the attraction of fluid elements occurs in the fastest way (Haller, 2001). Alternatively, recognizing that $\nabla\boldsymbol{v}(\boldsymbol{r},t) = \underline{\underline{A}}^{-1}\cdot\nabla_0\boldsymbol{v}_0(\boldsymbol{r}_0)$, where $\underline{\underline{A}}^{-1}$ is the inverse of $\underline{\underline{A}}$, and assuming the presence of a potential velocity field $\boldsymbol{v}_0(\boldsymbol{r}_0) = \nabla_0\phi(\boldsymbol{r}_0)$, one can do a similar analysis for the tensor $\nabla_0\nabla_0\phi$, noting that J in (46) becomes $J = \det(\underline{\underline{I}} + \tau\nabla_0\nabla_0\phi)$ (Shandarin and Zel'dovich, 1989).

As we are interested, however, in the dynamics of compressible vortex flows as well i.e. of non-potential flows, we shall choose a different way. We ask the question under which circumstances do density and vorticity experience a collapse for the first time. The answer is, when the hypersurface $J(\boldsymbol{r}_0,\tau)$ just touches tangentially the zero plane. Assuming that this happens at $\boldsymbol{r}_{0*},\tau_*$ we then have

$$J(\boldsymbol{r}_{0*},\tau_*) = 0\ , \tag{51a}$$

$$\nabla_0 J(\boldsymbol{r}_0,\tau_*)|_{\boldsymbol{r}_0=\boldsymbol{r}_{0*}} = 0\ . \tag{51b}$$

A discussion of this condition can be found in Schamel and Karimov (2000); Karimov and Schamel (2002). An example in 2D where such a prediction can be made and solved is shown in Fig. 6. It shows the initial streamlines of a converging ($x<0$) and diverging ($x>0$) flow and the path of the fluid element (dotted line) in the converging section that starts at $\tau = 0$ on the unit circle and collapses at τ_* at the lower diamond within the circle.

In 3D, using (45), (51b) can be written as

$$\tau\nabla_0 s_0 + \tau^2\nabla_0 d_0 + \tau^3\nabla_0 p_0 = 0 \tag{52}$$

which can also be formulated as

$$\underline{\underline{T}}\cdot\boldsymbol{\xi} = 0 \tag{53}$$

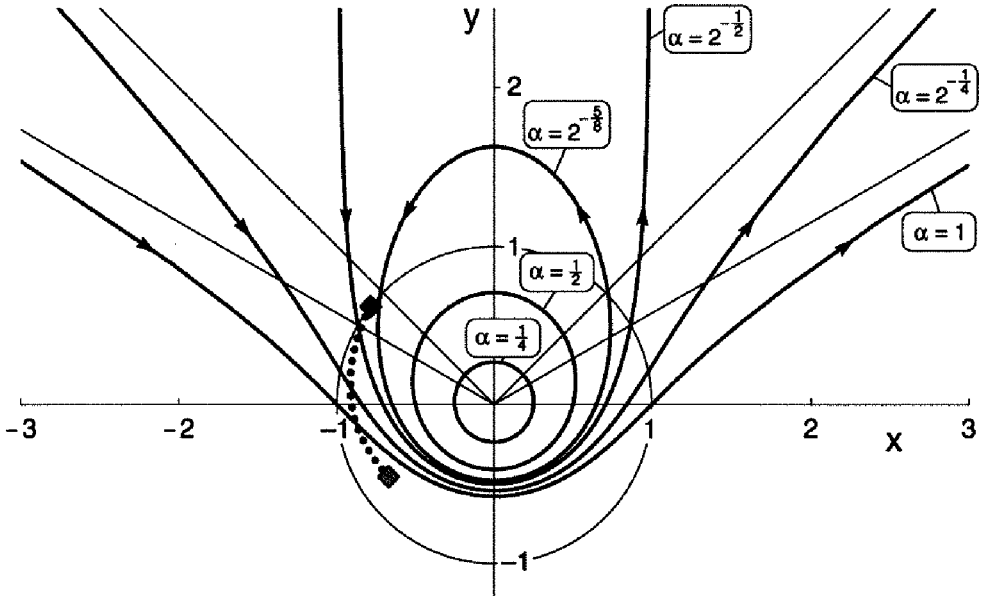

Fig. 6. Initial streamlines (thick solid lines) and trajectory of the fluid element that collapses first (dotted lines) (from Schamel and Karimov, 2000).

with

$$\underline{\underline{T}} := \nabla_0 \boldsymbol{\eta}, \quad \boldsymbol{\eta} := \begin{pmatrix} s_0 \\ d_0 \\ p_0 \end{pmatrix}, \quad \text{and} \quad \boldsymbol{\xi} := \begin{pmatrix} \tau \\ \tau^2 \\ \tau^3 \end{pmatrix}.$$

A nontrivial solution $\boldsymbol{\xi}_*$ to (53) requires that $\det \underline{\underline{T}} = 0$ at the critical point $\boldsymbol{r}_{0*}$. The latter is the Wronski determinant of the $\boldsymbol{\eta}$ field and its disappearance is satisfied if s_0, d_0 and p_0 are dependent functions, such as $d_0 = D(s_0)$, $p_0 = P(s_0)$. Evaluating these conditions in more detail (Karimov and Schamel, 2002), a variety of admissible solutions is found. One simple example is $D(s_0) = s_0^3/3$, $P(s_0) = (s_0/3)^3$ for which $J(\boldsymbol{r}_0, \tau) = (1 + \tau s_0(\boldsymbol{r}_0)/3)^3$, which is, however, non-generic as it implies a purely radially imploding flow for which a whole surface of initial fluid elements collapse simultaneously at $\tau_* = \min_{\boldsymbol{r}_0 \in \mathbb{R}^3}(-3/s_0)$. This example, in addition, shows that a spherically exploding flow can never experience a collapse, in 2D and 3D, if it is solely driven by convection.

More generic collapsing events in 2D and 3D are associated with collapses along lines and surfaces.

3.3. Large scale structures in the Universe—caustics

An interesting question arises how a convection driven ideal system behaves past the collapse i.e. for an intermediate time $t > t_*$ (but short enough before the final asymptotics takes place). In Section 2 we have given for 1D already two answers: either viscosity comes into play or multi-streaming develops in phase space. The first option has two advantages: one can stay in the hydrodynamic regime and it may serve as a model for mass concentration in the Universe.

If a viscosity term is included in the momentum equation, such as in (25) without the electric field term, we essentially have to deal with Burgers equation, coupled with the continuity equation. Our numerical result shown in Fig. 4 shows that at least for a certain period $t_* < t < t_M$ a strongly enhanced density peak exists, embedded in a low density environment. Switching from the ion expansion problem to the problem of mass inhomogeneity in the Universe, we recognize a similarity with the two proposed models, the so-called pancake model of Zel'dovich (Shandarin and Zel'dovich, 1989) and the adhesion or sticking model of Gurbatov and Saichev (Gurbatov et al., 1991). Both models rely on the observation made by Zel'dovich and others (see, e.g., Gurbatov et al., 1991) that primordial random density perturbations (of Gaussian type) in an Einstein–de Sitter cosmological model are described after the inflationary phase by the 3D ideal fluid equations given by (38a,b).

These two models predict the persistence of a density peak (clump) at x_*, the caustic, where for the first time the intersection of two trajectories occurs. We add that this is supported by the numerical simulations of Sack and Schamel (Sack and Schamel, 1987), as indicated in Fig. 4. In the Universe gravity will prevent this mass concentration from expansion such that a compact mass object representing cold sticky dust is born. In 2D and 3D pancakes resulting from gravitational instability (Shandarin and Zel'dovich, 1989) with different principal orientations will intersect and will create caustic lines with a still enhanced mass concentration which themselves may intersect to generate clumps of an again higher mass concentration. As a result the pancakes merge into a cellular and filament-like structure with voids in between which appears to be generic in 3D. This is seen as foam in 2D and 3D simulations (Shandarin and Zel'dovich, 1989; Gurbatov et al., 1991). The formation of large-scale structures after the baryon-photon decoupling in the early Universe is hence thought to be tracing the dynamics of cold dark matter in a rarefied medium formed by collisionless dust-like particles interacting only via Newtonian gravity. Thus, as it is rather probable that most of the mass in the Universe (about 90% or more) is composed of weakly interacting massive particles (wimps, such as neutralinos, ...), we have to deal mainly with the motion of a collisionless medium driven by advection up to caustic formation. That such a scenario may indeed explain large scale structures of our Universe as indicated by the following figure.

Fig. 7 shows the recent observation of a hot filamentary cloud of gas made by the Chandra X-ray observatory [http://chandra.harvard.edu]. An artists rendering illustrates how X-rays from a distant quasar dim as they pass through a cloud of the intergalactic gas. By measuring the amount of dimming due to oxygen and other elements in the cloud (see the spectrum of the quasar PKS 2155-304 in the inset) astronomers were able to estimate the temperature, density and mass of the absorbing gas cloud. This hot intergalactic gas ($T \simeq 3 \times 10^5$–$5 \times 10^{6^\circ}$C) appears to lie *like a fog in channels carved by rivers of gravity*. It is thought that this gas forms part of a gigantic system, or web, of hot gas and dark matter that defines the cosmic landscape. The hot gas part alone could contain more material than all the stars in the Universe. It can be used to trace and map the more massive dark matter component, and eventually to find out whether the total mass of our Universe is large enough to stop and to reverse the expansion initiated by the big bang.

We hence come to the perhaps surprising conclusion that the motion of self-gravitating matter in the expanding Universe may be like that of noninteracting dark matter moving by inertia. And finally we mention that the kind of structure in question may have been found in the spatial distribution of galaxies, clusters and superclusters of galaxies and huge voids in between, as well, in accordance with the so-called "bottom-up" scenario (Shandarin and Zel'dovich, 1989).

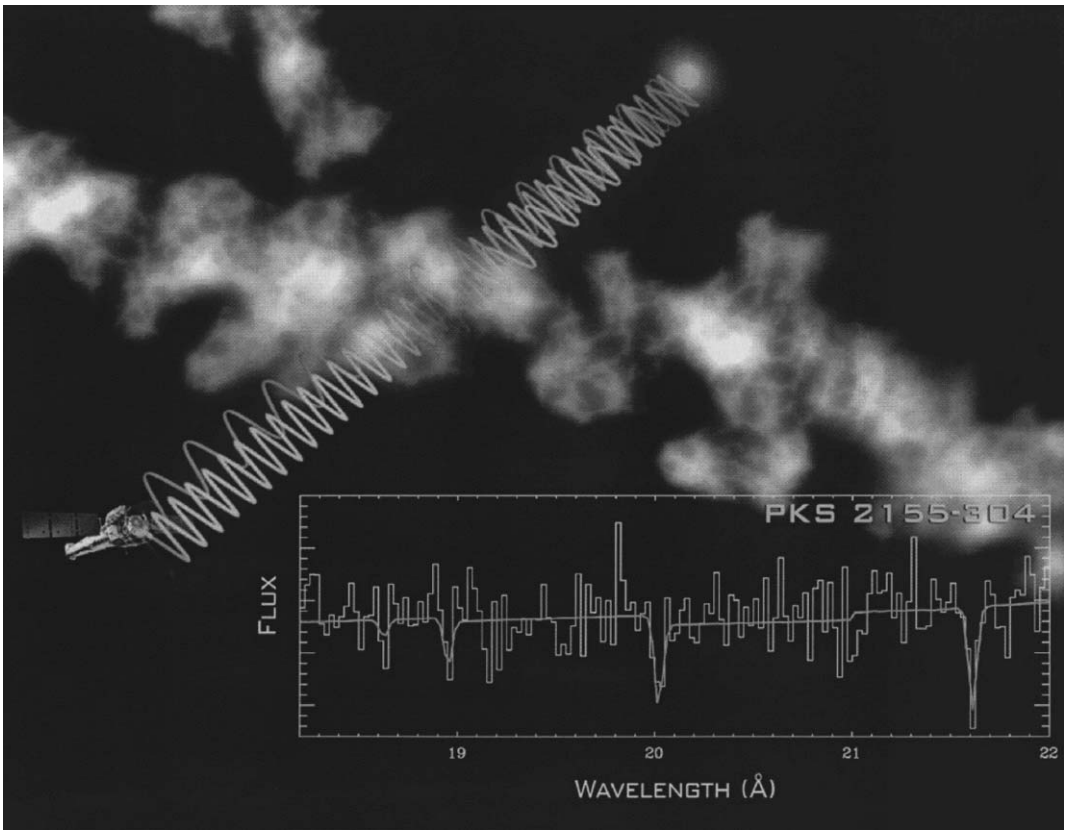

Fig. 7. A hot filamentary cloud of gas surrounding thin caustic regions of dark matter. An artist's rendering illustrates how X-rays from a distant quasar dim as they pass through a cloud of intergalactic gas. In the inset, the spectrum of the quasar PKS 2155-304 is shown, yielding information about the amount of dimming due to oxygen and other elements in the cloud (from Chandra X-ray observatory).

4. Collective diode dynamics

4.1. Modeling of ballistic electron transport

The next section is devoted to the electron transport in a planar diode bounded by two electrodes, an emitting electrode (cathode) at zero potential and a collecting electrode (anode) at an applied potential (see Fig. 8). Such a device, as simple as it is, can exhibit a variety of surprises despite the fact that it belongs to those devices with the longest history. For a review with respect to its DC solutions and their stability see Ender et al. (2000). Its importance in technology cannot be overestimated. It has a huge application potential with respect to the electron (particle) transport in vacuum diodes (triodes) and in nanoelectronic semiconductor diodes, to mention two of them.

We shall employ the Lagrangian description and derive with it some new results which have been hidden in the last century's diode research.

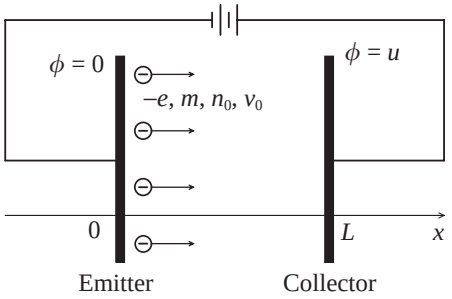

Fig. 8. Schematic of an electron vacuum diode.

The basic equations determining the collective electron dynamics in a diode are given in Eulerian space in the zero pressure limit by

$$\partial_t n + \partial_x(nv) = 0 \ , \tag{54a}$$

$$\partial_t v + v\partial_x v = -E \ , \tag{54b}$$

$$-\partial_x E = \alpha^2 n \tag{54c}$$

which represent continuity, momentum and Poisson's equation in dimensionless form. Density, velocity, length, time and electric field are normalized by the density n_0 and velocity v_0 of injected electrons, by the diode length L, by L/v_0 and by $m_e v_0^2/eL$, respectively, which are assumed to be constants. The parameter α in (54c) is given by

$$\alpha = \left(\frac{n_0 e^2 L^2}{\epsilon_0 m_e v_0^2}\right)^{1/2} \tag{55}$$

and is usually called the Pierce parameter. It increases with increasing density and diode length and with decreasing injection velocity, being one of the control parameters of the system. System (54) is supplemented by the boundary conditions

$$\begin{aligned} &n(0,t) = 1, \quad v(0,t) = 1 \ , \\ &\phi(0,t) = 0, \quad \phi(1,t) = V \end{aligned} \tag{56}$$

from which we get, using $E = -\partial_x \phi$, the potential condition

$$\int_0^1 \mathrm{d}x\, E(x,t) = -V \ . \tag{57}$$

Passing over to the Lagrangian description (Schamel and Bujarbarua, 1993) we introduce, in similarity to (15), the Lagrangian variable

$$t_0(x,t) := t - \int_0^x n(x',t)\,\mathrm{d}x' \ . \tag{58}$$

Assuming that (58) is invertible (at fixed t), we conclude that $x(t_0,t)$ represents the Eulerian coordinate x of a fluid element that was injected into the diode at $t = t_0$, so that we have $x(t_0,t_0) = 0$; t_0 is, hence, the injection time of an individual fluid element and serves as a Lagrangian coordinate

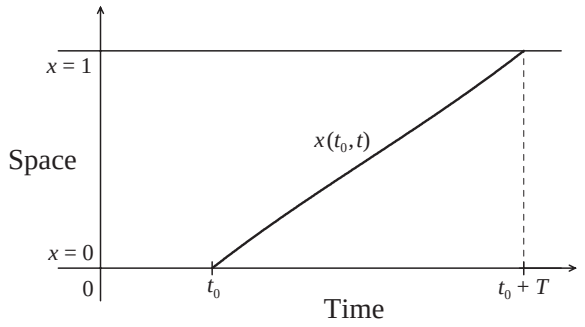

Fig. 9. A typical trajectory of an electron fluid element.

(label). In Fig. 9 a typical trajectory is drawn. It terminates at the anode ($x = 1$) at the time $t_0 + T$ where the electron (better the fluid element) is collected. T is hence the transit time of an electron.

Note that, as before, $t_0(x,t)$ is constant along the path of an electron fluid element and is hence a streamfunction. Making use of (56), (58) and of the identity

$$n(x,t) \equiv n(x(t_0,t),t) = \tilde{n}(t_0,t) \tag{59}$$

which relates the Eulerian with the Lagrangian density, we get for the transformation of the differentials (note that formally we have to add to (58) $\tau(x,t) \equiv t$ and consider τ and t_0 as the new L-variables; later τ is replaced by t).

$$\partial_x \to -\tilde{n}(t_0,t)\partial_{t_0} \ , \tag{60a}$$

$$\partial_t \to \partial_t + \tilde{n}(t_0,t)\tilde{v}(t_0,t)\partial_{t_0} \ . \tag{60b}$$

From (60) it easily follows $\mathrm{d}/\mathrm{d}t \equiv \partial_t + v\partial_x \to \partial_t$. It also holds in E-space $\partial_x t_0 = -n, \partial_t t_0 = nv$, such that the continuity equation is satisfied automatically, in analogy to (17). Therefore, in L-space, the basic set of Eqs. (54) becomes

$$\partial_t \tilde{n} - \tilde{n}^2 \partial_{t_0} \tilde{v} = 0 \ , \tag{61a}$$

$$\partial_t \tilde{v} = -\tilde{E} \ , \tag{61b}$$

$$\partial_{t_0} \tilde{E} = \alpha^2 \ . \tag{61c}$$

Furthermore, from the identity $t_0 = t_0(x(t_0,t),t)$ and from (58) we obtain by differentiation with respect to t_0 and t, respectively,

$$x'(t_0,t) = \frac{-1}{\tilde{n}(t_0,t)} \ , \tag{62a}$$

$$\dot{x}(t_0,t) = \tilde{v}(t_0,t) \ , \tag{62b}$$

where dot (dash) refers to $\partial_t(\partial_{t_0})$. Eqs. (61), (62) determine the evolution of the system in L-space subject to the initial conditions

$$x(t_0,t_0) = 0, \quad \dot{x}(t_0,t_0) = 1 \ . \tag{63}$$

The second relation in (63) comes from the identity $v(x(t_0,t),t) \equiv \tilde{v}(t_0,t)$ with the help of the first one in (63) and of $v(0,t) = 1$ from (56). It is easily seen that $\tilde{n}(t_0,t) = -1/x'(t_0,t)$ from (62a) provides a solution of (61a) by use of (62b).

A big advantage of the LFD is that (61c), the transformed Poisson equation, can be integrated directly,

$$\tilde{E}(t_0,t) = E_0 - \alpha^2(t - t_0) \ , \tag{64}$$

where E_0 stands for the electric field at the emitter. By use of (62b) and (64) the momentum equation (61b) can be written as

$$\ddot{x}(t_0,t) - \alpha^2(t - t_0) = -E_0 \ . \tag{65}$$

It constitutes together with the initial value condition (63) and the two boundary conditions

$$x(t_0, t_0 + T) = 1 \ , \tag{66a}$$

$$V = -\int_0^1 E(x,t)\,\mathrm{d}x \equiv -\int_t^{t-T} \tilde{E}(t_0,t)x'(t_0,t)\,\mathrm{d}t_0 = \int_t^{t-T} \ddot{x}(t_0,t)x'(t_0,t)\,\mathrm{d}t_0 \tag{66b}$$

the LFD of the electron dynamics in a diode. (66a) is the so-called transit time condition and (66b) the potential condition. In the derivation of the latter we made use of $\mathrm{d}x = x'(t_0,t)\,\mathrm{d}t_0$ at fixed t and of the fact that $x(t,t) = 0$ and $x(t-T,t) = 1$, which follows with $t_0 = t - T$ from (63) and (66a), respectively. The system has, therefore, two internally determined quantities, E_0 and T, and two external control parameters α and V.

4.2. DC solutions—the true space–charge-limited (SCL) current

Stationary solutions with no particle reflection can be found easily (Kolinsky and Schamel, 1997; Akimov et al., 2001): it holds $E_0(t) \equiv E_0 =$ const., and the dynamical quantities depend only on $q := t - t_0$, reflecting time invariance. The differentiation operators transform into: $\partial_t = \partial_q, \partial_{t_0} = -\partial_q$, and for the position of the electron fluid element we can write

$$\chi(q) := x(t_0,t) \ . \tag{67}$$

Eq. (65) then becomes

$$\chi''(q) - \alpha^2 q = -E_0 \tag{68}$$

which can be solved, using the boundary conditions (63) becoming $\chi(0) = 0, \chi'(0) = 1$, by

$$\chi(q) = \frac{1}{6}\alpha^2 q^3 - \frac{1}{2}E_0 q^2 + q \ . \tag{69}$$

The transit time condition (66a) then becomes $\chi(t) = 1$ and therefore

$$\frac{\alpha^2 T^3}{6} - \frac{E_0}{2}T^2 + T - 1 = 0 \ . \tag{70}$$

The potential condition (66b) becomes

$$V = \int_0^T \mathrm{d}q\, \chi'(q)\chi''(q) = \frac{1}{2}\,[\chi'(T)^2 - 1]$$

from which we get

$$\chi'(T) = \sqrt{1+2V}\ , \tag{71}$$

where the + sign has to be taken and $V > -1/2$ to guarantee absence of reflection. Differentiating (69) we get for (71)

$$\frac{\alpha^2 T^2}{2} - E_0 T + 1 = \sqrt{1+2V}\ . \tag{72}$$

There are, hence, two equations, (70) and (72), for the two unknown internal quantities E_0 and T.

Eliminating E_0 from (70) and (72) we get

$$-\frac{1}{12}\,\alpha^2 T^3 + \frac{T}{2}\,(1+\sqrt{1+2V}) - 1 = 0 \tag{73}$$

which determines the transit time $T(\alpha, V)$ in terms of α and V. An elimination of α from (70) and (72) yields

$$E_0 = \frac{2}{T}\,[2+\sqrt{1+2V}] - \frac{6}{T^2} \tag{74}$$

which gives via $T(\alpha, V)$ the emitter electric field $E_0(\alpha, V)$ in terms of α and V.

As a footnote we mention that in the vacuum limit $\alpha \to 0$ ($n_0 \to 0$) (73) yields $T=2/(1+\sqrt{1+2V})$ which inserted into (74) gives $E_0 = -V$. Our solution hence automatically includes the capacitor limit.

A thorough discussion of the cubic equation (73) shows (Akimov et al., 2001), that there is always a negative solution, $T_1 < 0$, which, however, is ruled out as a transit time. The other two solutions are real and positive, provided that

$$\alpha_{\mathrm{BF}} \leqslant \alpha \leqslant \alpha_{\mathrm{SCL}}\ , \tag{75}$$

where

$$\alpha_{\mathrm{BF}} := \frac{\sqrt{2}}{3}\,[1+\sqrt{1+2V}^{3/2}]\ , \tag{76a}$$

$$\alpha_{\mathrm{SCL}} := \frac{\sqrt{2}}{3}[1+\sqrt{1+2V}]^{3/2}\ . \tag{76b}$$

In this region we, therefore, have two solutions of our problem, for the transit time as well as for the emitter electric field E_0, whereas for $\alpha < \alpha_{\mathrm{BF}}$ only one of the two solutions exists.

Fig. 10 shows E_0 as a function of α for a fixed anode potential $V=2$. We recognize the two solutions, as just mentioned, called normal C and C-overlap (Fay et al., 1938), and a third one starting at $\alpha=\alpha_{\mathrm{BF}}$, which was not included in our analysis because for this solution particle reflection at the potential minimum, called the virtual cathode, had to be taken into account. We see a hysteresis type behavior. For $\alpha > \alpha_{\mathrm{SCL}}$ only the virtual cathode solution exists as a DC solution, which disappears when α is lowered at $\alpha=\alpha_{\mathrm{BF}}$, below which only the normal C solution exists. The C-overlap equilibrium turns out to be unstable. Both critical α's, α_{BF} and α_{SCL}, are bifurcation points. We denoted the

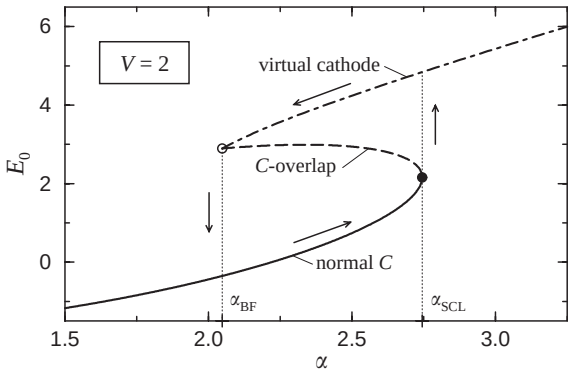

Fig. 10. Electric field at the emitter as a function of α for a given collector potential ($V = 2$). A hysteresis behavior is pointed out (from Akimov et al., 2001).

larger one by an index SCL since it is related with the maximum current—the space–charge-limited current—a diode can sustain.

To learn more about this current we return to dimensional quantities and introduce the current density J by

$$J = en_0v_0 \ . \tag{77}$$

Replacing n_0 by J in α we get from (55)

$$\alpha^2 = \frac{eJL^2}{\epsilon_0 m_e v_0^3} \tag{78}$$

which shows, that for fixed diode length L and fixed injection velocity v_0, J grows proportional to α^2. Maximum current is, hence, achieved when α equals α_{SCL}. With (76b) and using $V \equiv eU/m_e v_0^2$ we find

$$J_{SCL} = \frac{2\epsilon_0 m_e}{9eL^2}\left(v_0 + \sqrt{v_0^2 + \frac{2eU}{m_e}}\right)^3 \tag{79}$$

which we call the *true* SCL current. It is always larger than the one predicted by Child (1911) to which (79) reduces when the limit $U \to \infty$ or $v_0 \to 0$ ($n_0v_0 =$ const.) is taken, namely

$$J_{CL} = \frac{4}{9}\sqrt{\frac{2e}{m_e}}\epsilon_0 \frac{U^{3/2}}{L^2} \ . \tag{80}$$

For finite injection velocities and for not too large potential drops U, the Child law (80) is hence erroneous and must be replaced by (79). In addition, in an attempt to improve Child's law for finite injection velocities, Langmuir (1923) proposed to apply Child's law for the reduced distance and enhanced potential drop between the virtual cathode and the anode, corresponding to the onset of particle reflection. In this procedure the maximum current is defined by $\alpha = \alpha_{BF}$, and hence this Child–Langmuir current is still less than the true SCL current (Akimov et al., 2001). The correct SCL current is a result of an internal bifurcation and not due to an onset of electron reflection. For a more detailed discussion of other erroneous definitions of the space–charge-limit current we refer to Akimov et al. (2001).

Finally, we mention that the Child–Langmuir law as a SCL current remains valid in the case of field-emitted electrons, since in that case $v_0 = 0$ (Akimov et al., 2001). Hence, our Lagrangian analysis performed in a straightforward manner revealed a new quality of a diode, not yet found in the relevant textbooks about charge transport in bounded systems.

4.3. Collisional effects

Two further diode processes will be sketched to emphasize the potential strength of the method based on LFD. The last one will be the physics triggered by a sudden switching of the collector potential. Before that we investigate briefly the effect of a friction on the electron transport. We, hence, replace (54b) by

$$\partial_t v + v\partial_x v = -E - \nu v \ . \tag{81}$$

The Drude friction term in (81) models collisions with the background which may become important in high pressure discharge devices or in semi-conductor plasma devices of not too short basis lengths (otherwise the transport would still be ballistic as in many nanodevices).

At first we shall see that within the Euler description the problem is rendered unsolvable. Indeed, looking for steady state solutions, $\partial_t = 0$, and assuming that there exists a unique relationship, $v = v(\phi)$, such as in Riemann's analysis of gas dynamics, i.e. that v depends through ϕ on x from which follows $\partial_x v = v'(\phi)\partial_x\phi$, we get from (81)

$$v[v'(\phi) + \nu x'(\phi)] = 1 \ , \tag{82}$$

where $x'(\phi) = 1/\partial_x\phi|_{x=x(\phi)}$, which follows from the identity $x \equiv x(\phi(x))$, where $x(\phi)$ is the inversion of $\phi(x)$. Eq. (82) is Abel's equation of second kind, for which, however, no general solution is known, i.e. for a general unspecified function $x(\phi)$. Here, an attempt to solve our problem in Euler space would have to be given up.

In L-space, instead, a solution can be found (Akimov and Schamel, 2002). The momentum equation (65) is supplemented by a new term $\nu\dot{x}(t_0, t)$, whereas the transit time condition (66a) and potential condition (66b) remain unchanged. As the analysis shows, we again arrive at two conditions for E_0 and T [namely (19) and (23) in Akimov and Schamel (2002)] for given external parameters α, V and ν which can be solved numerically. Fig. 11 shows the emitter electric field E_0 as a function of the Pierce parameter α for several ν's at a fixed anode potential ($V = 1$). Qualitatively the situation with respect to possible DC solutions is as before ($\nu = 0$), which for comparison is included too. We see, how an increasing friction restricts the existence range of E_0. At $\nu = 12 \equiv \nu_{\max}(V = 1)$ both bifurcation states SCL and BF merge into one state. For any ν going beyond this maximum no true SCL solution can be found any longer. Electrons starting from the emitter experience such a strong friction that they will be reflected before reaching the collector (at finite V).

The analysis can also be applied to the field emission limit $E_0 \to 0, v_0 \to 0$, in which case, returning to dimensional quantities, the following SCL current is found, shown in Fig. 12. The ν dependence of the current density J normalized by the Child value J_{CL} is plotted for several values of the anode potential U. For $\nu \to 0$ the Child law (80) is recovered, becoming $J_{\mathrm{CL}} = A(4\sqrt{2}/9)(U^{3/2}/L^2)$

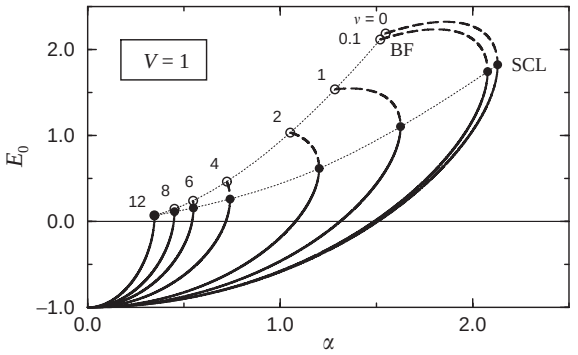

Fig. 11. The emitter electric field as a function of α for $V = 1$ and several values of v. Note that only the normal C and the C-overlap branches are shown (from Akimov and Schamel, 2002).

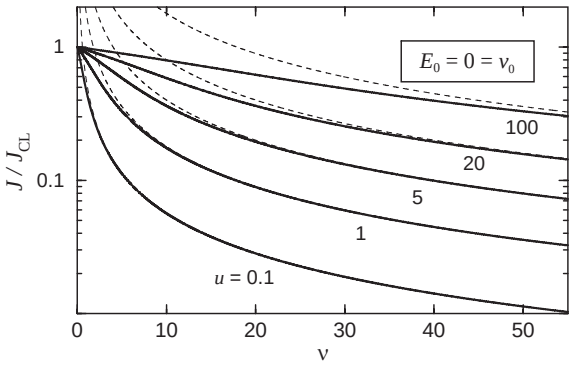

Fig. 12. SCL current in the Child–Langmuir limit ($E_0 = 0 = v_0$) normalized by J_{CL} for several values of U as a function of v. Dashed curves refer to the Mott–Gurney SCL current (from Akimov and Schamel, 2002).

with $A \equiv \epsilon_0 \sqrt{e/m_e}$, whereas for $v \to \infty$ any curve approximates the asymptote given by

$$J_{MG} = A \frac{9U^2}{8vL^3} \tag{83}$$

representing the so-called Mott–Gurney law well-known in semiconductor physics being valid within the drift approximation.

The true SCL current–voltage characteristics for arbitrary v_0 which comprises both effects, inertia as well as frictional effects, can be found as well (see Akimov and Schamel, 2002).

We conclude, that the competition between inertia and friction in the electron momentum equation can be completely resolved within the LFD only, allowing the bridging between ballistic and drift dominated transport.

4.4. Transients triggered by switching

And last but not least the LFD is applied to a rapidly t-dependent diode problem, namely the electron response triggered by a sudden switching of the collector potential. The set of equations to be solved is that of (54)–(57) with the difference that V is now given by

$$V(t) = \Delta V\theta(t) \tag{84}$$

with $|\Delta V| \ll 1$, and

$$\theta(t) = \begin{cases} 0 & t < 0 \\ 1 & t > 0 \end{cases}$$

being the Heaviside function. For $t < 0$ the diode is assumed to be short circuited and in a stable DC state on the normal C branch (see Section 4.2). The collector potential is switched at $t = 0$ to $\Delta V > 0$. We show that this switch causes transient processes in the electron dynamics which can be understood completely by means of the LFD (Akimov et al., 2003).

If T_0 and E_{00} are the equilibrium transit time and emitter electric field before switching, respectively, a solution can be found by assuming

$$x(t_0, t) = \chi(q) + x_1(t_0, t)\theta(t) \ , \tag{85a}$$

$$E_0(t) = E_{00} + E_1(t)\theta(t) \ , \tag{85b}$$

$$T(t) = T_0 + T_1(t)\theta(t) \tag{85c}$$

with smallness quantities indexed by 1. Linearizing the governing set of equations, one can show (Akimov et al., 2003) that for particles emitted at $-T_0 \leqslant t_0 < 0$, the so-called "old" particles, it holds for the deviation of their trajectory

$$x_1(t_0, t) = -\int_0^t \mathrm{d}t'(t - t')E_1(t') \ , \tag{86}$$

whereas for "fresh" particles, emitted at $t_0 \geqslant 0$, we have

$$x_1(t_0, t) = -\int_{t_0}^t \mathrm{d}t'(t - t')E_1(t') \ . \tag{87}$$

$E_1(t)$ satisfies a third order, retarded differential equation given by

$$\dddot{E}(t) - T_0\dot{E}_1(t) + 2E_1(t) = 2E_1(t - T_0)\theta(t - T_0) + T_0[\dot{E}_1(t - T_0)\theta(t - T_0) + E_1(t - T_0)\delta(t - T_0)] \ , \tag{88}$$

where $\delta(t) = \dot{\theta}(t)$ is the delta function. Eq. (88) can be solved interval-wise, i.e. the solution $E_1^{(1)}$ in the first interval, $0 \leqslant t < T_0$, determines the solution $E_1^{(2)}$ in the second interval, $T_0 \leqslant t < 2T_0$, and so on.

Fig. 13 shows $E_1(t)$ for $\Delta V = 0.02, \alpha = 1$ ($T_0 = 1.1157$) in the first two intervals. Open circles are obtained by a Vlasov simulation of the dynamics whereas solid line represents the analytical result. We see an exact agreement. At $t = 0$, $E_1(t)$ suddenly jumps to a small negative value ($E_0(t)$, which

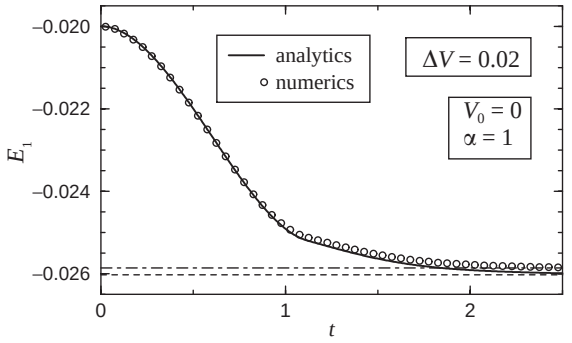

Fig. 13. Emitter electric field perturbation as a function of time. Analytic solution (solid line), numerical solution (open circles) (from Akimov et al., 2003).

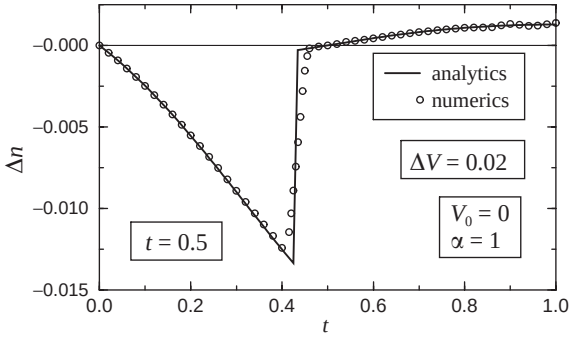

Fig. 14. The spatial dependence of the density perturbation at $t = 0.5$. Analytic solution (solid line), numerical solution (open circles) (from Akimov et al., 2003).

is positive, decreases) and approaches the new, asymptotic DC value essentially within the first two intervals.

A snapshot of Δn, the perturbed density in E-space, is shown in Fig. 14. We see that a rarefaction pulse propagates with a sharp front across the diode. Old particles to the right of the front are just leaving the diode whereas fresh particles, injected after the switch, have already experienced a decreased decelerating electric field and propagate faster with a decreased density.

Finally, Fig. 15 shows the current density at the collector as a function of time, both analytically and numerically. We recognize a current peak at $t = T_0$ which marks the instant when the last injected old particle leaves the diode. The current is still slightly perturbed in the second interval since it is composed of fresh particles. The latter particles experience an altered space charge distribution when they enter into the diode which is due to the strong response of the old particles to the switching event. Note that, since the injection conditions are unchanged, J should approach unity as $t \to \infty$, as it does.

Again a perfect agreement between theory, based on LFD, and numerics can be stated. With it a complete understanding of the transient nature of the electron dynamics triggered by a weak voltage switching has been achieved. For more details see Akimov et al. (2003).

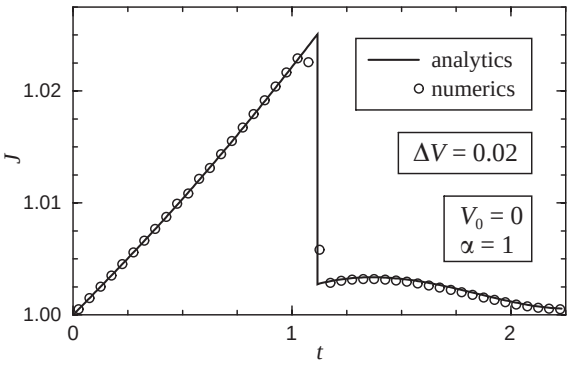

Fig. 15. The current density at the collector as a function of time. Analytic solution (solid line), numerical solution (open circles) (from Akimov et al., 2003).

Ions have been neglected so far, as can be seen from (54), which describes the electron dynamics of a pure electron diode (also referred to as Bursian diode). Plasma diodes, on the other hand, in which ions are taken into account and hence can achieve states closer to quasineutrality, are of interest by its own as important physical systems can be accounted for. The simplest of such diodes is the classical Pierce diode (Pierce, 1944; Godfrey, 1987) where the mean electron density equals that of the ions which are considered immobile.

Examples for which extended Pierce diodes generalized by a mobile ion background can be utilized are collective effects accelerators, high power microwave sources, inertial confinement fusion drivers, cosmic plasma flows, or *p-i-n* diodes in semiconductors, to mention some of them (Schamel and Maslov, 1993). Finite ion masses as well as finite ion injection velocities give rise to new degrees of freedom or, expressed in different words, to new channels of destabilization. Pierce-like diodes, for instance, can become unstable by oscillatory modes on electronic time scales already. Without going into detail, we mention that this can again be treated favorably and in some cases solely by the LFD by establishing and solving linear dispersion relations (Schamel and Maslov, 1993; Kolinsky and Schamel, 1994, 1995; Ender et al., 2000).

5. Collapses and strange solitons in current carrying plasmas

5.1. Modeling of current carrying plasmas

In our last section, we consider current driven plasmas as often met under laboratory and extraterrestric conditions. As in Section 2.1 we adopt a two fluid model in which the evolution is assumed to be governed by the ions. This implies that electrons behave as a quasi-stationary fluid described by an equation of state, which follows from mass conservation and the Bernoulli law. Using the same normalization as in Section 2.1, we get as the basic set of equations in 1D, following Schamel and Hassan (1997),

$$\partial_t n + \partial_x(nv) = 0 \ , \tag{89a}$$

$$\partial_t v + v\,\partial_x v = -\partial_x \phi - \Theta^{-1}\partial_x \ln n \ , \tag{89b}$$

$$\partial_x^2 \phi = n_e(\phi) - n \ , \tag{89c}$$

$$\phi(n_e) = \ln n_e + \frac{1}{2} v_0^2 (n_e^{-2} - 1) \ , \tag{89d}$$

where $\Theta := T_e/T_i$ with $T_s = \text{const}$, $s = e, i$ (isothermal limit).

The (unperturbed) drift velocity of the electrons is given by v_0 in units of the electron thermal velocity. In case of vanishing drift (current), the Boltzmann law (2) is recovered from (89d), which hence represents a generalized equation of state $n_e(\phi)$ or $\phi(n_e)$, respectively.

In case quasineutrality represents a valid approximation, system (89) reduces to

$$\partial_t n + \partial_x (nv) = 0 \ , \tag{90a}$$

$$\partial_t v + v\,\partial_x v = -\partial_x \left[\lambda \ln n + \frac{v_0^2}{2n^2} \right] \tag{90b}$$

with $\lambda := 1 + \Theta^{-1}$ representing the thermal effect. A linear treatment of the latter system (Belova et al., 1980; Galeev et al., 1981) reveals an aperiodic instability, provided that v_0^2 exceeds λ. For the general system (89), however, the aperiodic instability is further restricted by $k^2 < (v_0^2 - 1)^{-1}$, where k is the wavevector. Therefore, for sufficiently large drift velocities of the order of the electron thermal velocity—in the so-called Buneman unstable range (Mantei et al., 1976)—linear waves in the long wavelength limit exhibit an aperiodic growth raising the question about the ultimate nonlinear behavior of a wave packet in course of time.

This problem, again, can be innovatively investigated by the Lagrangian fluid description.

5.2. *Quasineutral wave equation—self-similar solution*

First, we concentrate on the quasineutral system (90) and formulate the equations in the Lagrangian fluid description. Introducing the Lagrangian mass variable η, Eq. (15), and the specific volume $V(\eta, \tau) = n(\eta, \tau)^{-1}$, we can, as in Section 2.5, derive a scalar wave equation. From (90a,b) we get with ∂_x being replaced by $(1/V)\,\partial_\eta$:

$$\dot{V}(\eta, \tau) = v'(\eta, \tau) \ ,$$

$$\dot{v}(\eta, \tau) = \left[\frac{\lambda}{V^2} - v_0^2 \right] V'(\eta, \tau)$$

which can be combined in the scalar wave equation:

$$\ddot{V} + v_0^2 V'' = \lambda [V^{-2} V']' \ , \tag{91}$$

where a dash again refers to ∂_η.

A simple self-similar solution of (91) is found by Schamel and Hassan (1997)

$$V(\eta, \tau) = \frac{v_0 \tau}{\eta^2 + v_0^2 \tau^2} \ . \tag{92}$$

To learn what (92) predicts and when (92) is applicable we return to the Eulerian fluid description. Using (92), we get by an η-integration of (20c) the trajectory of a Lagrangian ion fluid element

$$x(\eta,\tau) = -\mathrm{arctg}\left(\frac{\eta}{v_0\tau}\right). \tag{93}$$

Its inversion yields then in Eulerian space

$$\eta(x,t) = -(v_0 t)\,\mathrm{tg}\,x \tag{94}$$

and by application of (17) one finds

$$n(x,t) = \frac{v_0 t}{\cos^2 x}, \quad v(x,t) = -\frac{\sin 2x}{2t} \tag{95}$$

a solution which has been found earlier by Belova et al. (1980) and Galeev et al. (1981).

This solution predicts a density rarefaction collapse (or a blow-up of the specific volume V) in the final stage of the evolution, when $t \to 0_+$. (Note that due to translational invariance in time $t \to t^* - t$ of (90b), we have shifted the time of singularity to the origin.) The leading term in the electric potential, as $t \to 0_+$, is found from (89d) in quasineutral approximation, $n_e = n_i$, and becomes

$$\phi(x,t) = \frac{\cos^4 x}{2t^2}\ , \tag{96}$$

where we used the fact that the second term on the RHS of (89d) is large in comparison with the first term. Similarly, from the RHS of (90b) we learn that the first term stemming essentially from the thermal effect becomes negligibly small near collapse, which formally can be replaced by letting $\lambda \to 0$. In this limit, however, the RHS of (91) vanishes and (92) represents a true solution of the scalar wave equation (91). The validity of (92), hence, requires $\eta \to 0$ as $\tau \to 0_+$, in which case we get $\eta/\tau \to O(1)$ and $V(\eta,\tau) \sim \tau^{-1} \to \infty$.

One is, hence, tempted to make following conclusion. If a density rarefaction is triggered by some mechanism, as seen e.g. in the experiment of Takeda et al. (1995), it should be governed in its last stage, preceding the collapse, by the self-similar solution (92) in the Lagrangian and by Eqs. (95) and (96) in the Eulerian space. With other words, a local density depression and an associated singularity in the specific volume should occur in finite time. This explosive process hence seems to be a possible collapse scenario of a current-driven plasma as stated in Belova et al. (1980) and Galeev et al. (1981). During this event, effects such as thermal pressure force and electron reflection ($\phi > 0\,!$) would turn out to be negligible. Note that due to (95) this rarefaction type of collapse would require a nonvanishing current (drift velocity). Moreover, although it is the electric potential (96) which exhibits the strongest singularity, behaving like $\phi \sim t^{-2}$ near $x \approx x_* \equiv 0$, the corresponding electric field would have no influence in the final collapse phase, as it disappears.

This interpretation, however, ignores the possibility of charge separation in a plasma which inevitably would come into play in the final stage of the collapse. In Section 5.3 we shall show that this is indeed the case with the consequence that this type of collapse is in fact ruled out by charge separation.

Returning to charge neutrality, we next show that there exists another possible collapse scenario. This second one is found by taking the thermal effect into account, i.e. by solving the scalar wave

equation (91) without the proviso of $\lambda \to 0$. A self-similar solution valid in the limit $\tau \to 0_+$ is found (Schamel and Hassan, 1997) by

$$V(\eta,\tau) = \frac{\tau}{\xi}[1 + \xi^{-1/2}(A\,\xi^{\kappa} + B\,\xi^{-\kappa})\,\tau + \cdots] > 0\ , \tag{97}$$

where $\xi := \alpha + \beta\eta$ and $\kappa := \frac{1}{2}\,[1 + 8/(\lambda\beta^2)]^{1/2}$; α, β, A, and B being constants.

For the Lagrangian trajectory we get by an η-integration of (20c), using this time equation (97),

$$x(\eta,\tau) = x_* + \frac{\tau}{\beta}\ln\left(1 + \frac{\beta\eta}{\alpha}\right)\ , \tag{98}$$

where higher order effects have already been dropped and x_* is a constant, representing again the spatial location of the singularity (as seen later).

For the Eulerian stream function $\eta(x,t)$ we get by inversion of (98), replacing τ by $t_* - t$,

$$\eta(x,t) = \frac{\alpha}{\beta}\left[\exp\frac{\beta(x - x_*)}{t_* - t} - 1\right] \tag{99}$$

from which we obtain by application of (17) in the vicinity of the singular point $x = x_*$

$$n(x,t) = \frac{\alpha}{t_* - t}\ , \tag{100a}$$

$$v(x,t) = \frac{x_* - x}{t_* - t}\ , \tag{100b}$$

$$\phi(x,t) = -\ln(t_* - t)\ , \tag{100c}$$

where the latter is again found in the lowest order from (89d) using quasineutrality.

We hence arrive at the solution (18) of Section 2.4 which implies density bunching as $t \to t_{*-}$. In this wave breaking scenario thermal pressure, electric field, and finite current effects turn out to be negligible. Note again that (19b), the ion momentum equation without any force term, is almost trivially satisfied by (100).

We mention that for both explosive processes only the final stage of the evolution can be described. The question of attraction i.e. which type of collapse is preferred by the system is out of the scope of a self-similar analysis as is the prediction of x_* and t_*, the coordinates of the singularity. Another important question is whether charge separation can prevent the ion fluid from collapsing. This is one of the topics to be studied in the final section.

5.3. Dynamics under charge separation—strange solitons

To get further insight into the ion dynamics in case of a current driven plasma we have to consult and investigate the full system (89).

First we cast this system into the Lagrangian form of fluid description. Making use of the specific volume $V(\eta,\tau) = n^{-1}(\eta,\tau)$, of the mass conservation $\dot{V}(\eta,\tau) = v'(\eta,\tau)$ [see Eqs. (20a) and (20c)], and of the ion momentum equation (89b)

$$\dot{v}(\eta,\tau) = -\frac{1}{V}\,[\phi(\eta,\tau) - \Theta^{-1}\ln V(\eta,\tau)]'\ ,$$

we get by combining both equations

$$\ddot{V} + [V^{-1}\phi']' = \Theta^{-1}[V^{-2}V']' \ . \tag{101a}$$

Poisson's equation (89c), on the other hand, reads

$$[V^{-1}\phi']' = n_e V - 1 \ , \tag{101b}$$

and from the equation of state (89d) we get by differentiation

$$\phi' = n_e^{-1}[1 - v_0^2 n_e^{-2}]\, n_e' \ . \tag{101c}$$

Substituting (101b) into (101a) and (101c) into (101b) and introducing the specific volume of the electron fluid by

$$\mathscr{U}(\eta,\tau) := n_e^{-1}(\eta,\tau) \tag{102}$$

we get the following coupled system

$$\ddot{V} + \mathscr{U}^{-1}V - 1 = \Theta^{-1}[V^{-2}V']' \ , \tag{103a}$$

$$\left[\frac{\mathscr{U}'}{\mathscr{U}V}(v_0^2\mathscr{U}^2 - 1)\right]' = \frac{V}{\mathscr{U}} - 1 \tag{103b}$$

which represents the Eulerian system (89) in its full generality in Lagrangian space.

First, let us apply a self-similar analysis to system (103). It can be shown (Schamel and Hassan, 1997) that a solution such as (92) for V and $\mathscr{U}$ does not exist for this full system. Therefore, the density rarefaction or cavity collapse is ruled out by charge separation. This seems not to be surprising, since one can argue that charge separation introduces an intrinsic length scale, the Debye length, which opposes the similarity principle, namely that the typical length scale vanishes with τ.

Hence, the explosive formation of a plasma cavity, as proposed by the Russian authors Belova et al. (1980) and Galeev et al. (1981), cannot take place in a real plasma in hydrodynamic description because of charge separation. Some other physical phenomenon, such as hf-field trapping in an electrostatic hole structure (Schamel and Maslov, 1999), has to be invoked to account for cavity formation seen in the experiment of Takeda et al. (1995).

To find out whether the second, the bunching singularity, is admitted by the system we make the ansatz (Schamel and Hassan, 1997)

$$V(\eta,\tau) = \tau\, G(\eta,\tau), \quad \mathscr{U}(\eta,\tau) = \tau\, H(\eta,\tau)$$

and get

$$2\dot{G} + \tau\ddot{G} + H^{-1}G - 1 = \Theta^{-1}\tau^{-1}[G'G^{-2}]' \ , \tag{104a}$$

$$\left[\frac{H'}{GH}(v_0^2\tau^2H^2 - 1)\right]' = \tau\left(\frac{G}{H} - 1\right) \ . \tag{104b}$$

If G and H together with their derivatives are quantities of $O(1)$, the leading terms G_0 and H_0 of G and H, respectively, have to satisfy in the limit $\tau \to 0_+$

$$[G_0'G_0^{-2}]' = 0, \quad [H_0'G_0^{-1}H_0^{-1}]' = 0 \ ,$$

the general solution of which becomes

$$G_0(\eta) = (\alpha + \beta\eta)^{-1}, \quad H_0(\eta) = (\alpha + \beta\eta)^{-r} \ ,$$

where r is an arbitrary exponent. The first part is, however, nothing else but the leading part of (97) and hence the ion density behaves like $n(x,t) = \alpha/(t_* - t)$, as in (100a), whereas for the electron density it holds $n_e(x,t) = \alpha^r/(t_* - t)$, noting that $\phi(x,t) = -\ln(t_* - t)$ and $E(x,t) = 0$ in leading order. Since the electric field does not contribute in the final stage of wave collapse, even if charge separation is taken into account, we conclude that the second type of collapse, the density bunching singularity, is not arrested by charge separation and hence applies for the full system, as well. The usual Debye length argument can obviously not be transferred to the wave breaking scenario as the effect of the electric field disappears when $t \to t_{*-}$. Other physical mechanisms, such as ion kinetic effects, have to be invoked to avoid this type of singularity.

As generally known, besides collapses there exist further nonlinear solutions of a given system, such as equilibria. Especially, in linearly unstable systems saturation by nonlinearity may provide such a state. This possibility is explored further in our last investigation.

Just above threshold of linear instability, a weak nonlinear analysis appears to be meaningful, i.e. we can set

$$V = 1 - v, \quad \mathscr{U} = 1 - u \tag{105}$$

with v and u being smallness quantities. Insertion of (105) into (103) yields the corresponding system in terms of v and u. Assuming an $(\eta - M\tau)$-dependence of both quantities (i.e. stationarity in the wave frame), where M is the not yet known Mach number, system (103) can be written in the form

$$v'N(v) + u'M(v,u) = 0 \ , \tag{106a}$$

$$v''N(v) + (v-u)(1+u) = 2\Theta^{-1}v'^2 \ , \tag{106b}$$

where

$$N(v) := M^2 - \Theta^{-1}(1+2v) \ , \tag{106c}$$

$$M(v,u) := (v_0^2 - 1)(1+v) - (v_0^2 + 1)u \tag{106d}$$

and a prime denotes differentiation with respect to η, as before.

An integration constant was set to zero, corresponding to a localized solitary wave solution we are looking for. Eq. (106b) can be used to eliminate u in terms of v

$$u = -\tfrac{1}{2}(1-v) + \sqrt{\tfrac{1}{4}(1-v)^2 + v''N(v) - 2\Theta^{-1}v'^2 + v} \ ,$$

where the $+$ sign of the square root was chosen to let $u \to 0$ if $v \to 0$.

Using the smallness of v, we get by Taylor expansion

$$u = v + \tilde{m}v'' - \tilde{m}^2(v'')^2 - (\tilde{m} + 2\Theta^{-1})vv'' - 2\Theta^{-1}(v')^2 \ , \tag{107}$$

where $\tilde{m}$ is defined by

$$\tilde{m} := M^2 - \Theta^{-1} \ . \tag{108}$$

We look for a weak amplitude solution just above threshold and assume the following scaling

$$(v_0^2 - \lambda),\ (v_0^2 - 1),\ \Theta^{-1},\ M^2 \ \approx\ O(\varepsilon) \ , \tag{109}$$

where $\varepsilon \ll 1$ is a measure of the deviation from threshold.

The last scaling hypothesis in (109) is in accordance with the fact that we have linearly an aperiodic instability implying zero phase velocity (lack of acoustic waves). With the scaling hypothesis (109) we get by substituting (107) into (106a), keeping only terms up to $O(\varepsilon^2)$

$$\begin{aligned} &v'(\tilde{m} - 2\Theta^{-1}v) + (v_0^2 - 1)[(v + \tilde{m}v'')' + vv'] \\ &\quad = (v_0^2 + 1)[v(v + \tilde{m}v'')' + \tilde{m}v'v''] \ . \end{aligned} \tag{110}$$

If we, in addition, adopt the scaling $v \approx O(\varepsilon^2)$ and $\partial_\eta \approx O(1)$, this equation can further be simplified to

$$(\tilde{m} + v_0^2 - 1)v' - (v_0^2 + 1)vv' + \tilde{m}(v_0^2 - 1)v''' = 0 \tag{111}$$

which is an equation of $O(\varepsilon^4)$. Using the boundary condition $v \to 0$ as $v'' \to 0$, we find by integration

$$\tilde{m}(v_0^2 - 1)v'' + (\tilde{m} + v_0^2 - 1)v - \frac{1}{2}(v_0^2 + 1)v^2 = 0 \ . \tag{112}$$

This equation can be solved by use of the classical potential method, namely, by writing (112) as $v'' = -\Upsilon'(v)$ which has the form of a classical conservative equation of motion. The classical potential $\Upsilon(v)$ is then found with $\Upsilon(0) = 0$ to be

$$-\Upsilon(v) = \frac{1}{|\tilde{m}|(v_0^2 - 1)}\left[(\tilde{m} + v_0^2 - 1)\frac{v^2}{2} - \frac{(v_0^2 + 1)}{6}v^3\right] \ . \tag{113}$$

A necessary requirement for a solution is that $\Upsilon(v)$ is negative and has a negative curvature at $v = 0$. This yields to

$$0 < -\tilde{m} < v_0^2 - 1 \ . \tag{114}$$

The second necessary condition for the existence of a solution, $\Upsilon(v_M) = 0$, gives the nonlinear dispersion relation

$$v_M = \frac{3(\tilde{m} + v_0^2 - 1)}{v_0^2 + 1} \ . \tag{115}$$

It determines the Mach number M via (108) as a function of the wave amplitude v_M.

Making use of (115), we can rewrite the classical potential (113) which then becomes

$$-\Upsilon(v) = Cv^2(v_M - v) \tag{116}$$

with $C := (v_0^2+1)/[6|\tilde{m}|(v_0^2-1)]$. Integration of the corresponding "energy" law $\frac{1}{2}(v')^2 + \Upsilon(v) = 0$, then yields

$$v(\eta) = v_M \operatorname{sech}^2\left(\sqrt{\frac{v_M C}{2}}\,\eta\right) \tag{117}$$

which gives the desired soliton solution. It has the shape of a hydrodynamic Korteweg–de Vries (KdV) soliton but with unusual scaling properties otherwise. This is why we call it strange soliton. Its extraordinary features are seen as follows. Evaluating the nonlinear dispersion relation (115) we find with $\epsilon := (v_0^2-1)(3v_0^2-1)^{-1}$, which is $O(\varepsilon)$,

$$M^2 = \Theta^{-1} - 2\epsilon(1+3\epsilon) + \frac{2}{3}v_M \tag{118}$$

being of $O(\varepsilon)$, as assumed. The solitary structure is, hence, almost nonpropagating in the laboratory frame and exists due to weak nonlinearity and weak instability.

Since v_M is $O(\varepsilon)$ we see from the definition of C that $v_M C$ is $O(1)$ and hence the width $\Delta \sim (v_M C)^{-1/2}$ of the solitary hump is of order unity. Denoting the small soliton amplitude by $\delta := v_M \sim O(\varepsilon^2)$ we hence get

$$M \sim O(\delta^{1/4}), \quad \Delta \sim O(1)\ ,$$

whereas an ordinary KdV-soliton would scale like $M \sim O(1)$, $\Delta \sim O(\delta^{-1/2})$ (in the laboratory frame).

Another unusual property is that in the present case the electric potential ϕ scales as $\phi \sim O(\delta^{3/2})$ in contrast to $\phi \sim O(\delta)$ of a KdV-soliton. In addition, ϕ which turns out to be negative has an opposite polarity related to the positive density perturbation opposite to a KdV-soliton, where both polarities are the same.

We note that also the second requirement for linear instability is satisfied, $k^2 < (v_0^2-1)^{-1} \sim O(\varepsilon^{-1})$ since $k^2 \sim \Delta^{-2} \approx O(1)$. The adjective "strange" is hence justified since, besides the unusual scaling properties, there exists no linear wave descendant to this solitary structure in contrast to the acoustic waves in the case of KdV-solitons, where the nonlinear steepening is balanced by dispersion, giving rise to the KdV-soliton. Obviously, linear wave theory does not necessarily provide a proper basis for structure formation processes, as often met in ideal, i.e., nondissipative fluids and plasmas. It can, at best, only give a hint where one may be successful in the search for new nonlinear structures.

We mention parenthetically that in a parametrically driven water filled wave guide a similar phenomenon of a nonpropagating hydrodynamic soliton could be observed experimentally for shallow water waves (Wu et al., 1984).

In conclusion, a current-driven, weakly Buneman unstable plasma in the small T_i regime admits a new class of solitons which look like a hydrodynamic KdV soliton but are slowly propagating, have an amplitude independent width of order unity and an opposite polarity between density and

electric potential variation, properties which hold in the Lagrangian as well as in the Eulerian frame of description.

The detection of this strange soliton and of the nonexistence of a rarefaction density collapse due to charge separation was made feasible by a Lagrangian analysis of the two coupled scalar wave equations (103).

This section, hence, provides another proof of the importance and innovative potential of the Lagrangian fluid description.

6. Summary and conclusions

An exploration of four dynamical processes of compressible dilute media based on the Lagrangian fluid description (LFD) was presented, showing the potential strength of this method in relationship to an Eulerian treatment.

In the fast ion blow-off of a laser produced, expanding plasma, where a complete analytical solution of the problem is absent, it was the use of a Lagrangian code and of a Lagrangian description of the governing equations based on the Lagrangian mass variable that allowed us to interprete the fast ion peak seen in experiments. It is a relic of a wave breaking scenario in the early stage of inviscid plasma expansion followed by a viscous stabilization of the singularity in terms of a finite, narrow, supersonic density clump.

In the purely convection driven motion of a compressible gas without internal forces a solution is available up to the formation of singularities. The latter appears in form of caustics in 2D and 3D which may mimic the motion of a non-interacting gravitating medium in the post inflationary stage of our expanding Universe, followed by the motion of cold dust under the action of gravity in the later stage.

In the diode physics with its high potential in technology the use of LFD could fed new light into some processes, such as the correct definition (and physical interpretation) of the maximum current limited by space charge, the competition between inertia and friction terms in the electron equation of motion (bridging ballistic and drift dominated transport) or the transient processes triggered by the switching of the collector potential.

In a current driven plasma the physics was shown to be governed in LFD by a scalar wave equation in the quasineutral and by two coupled wave equations in the general case of charge separation. The quasineutral scalar wave equation predicts two kinds of singular processes, a density cavity and a density bunching collapse, seen by a self-similar analysis. Whereas charge separation is shown to rule out the rarefaction collapse, the second bunching (or wave breaking) collapse was proven to survive in a more general charge nonneutral hydrodynamic plasma. Moreover, a new type of a hydrodynamic soliton with unusual scaling properties could be detected, which has no reference to linear wave propagation.

In this report we drew attention to the selfgeneration of coherent structures in laminar flows. In turbulent, incompressible flows the situation is quite comparable. Recent progress in the analytical (Ottino, 1990; Bohr et al., 1998 and references therein) and numerical (Yeung, 2002 and references therein) treatment of turbulent mixing flows has pointed out the preferential role of the Lagrangian flow description. It is the Lagrangian point of view which seems to be best suited to deal with chaotic advection as stretching and folding of material lines and surfaces are relying on the properties

of fluid particle trajectories. Furthermore, the resurgence in Lagrangian experimental measurements which use silicon strip detectors as optical imaging elements capable of handling data rates up to 70 000 (LaPorta et al., 2001), emphasizes the high potential LFD has.

In either case it is the nonlinear character of the phenomena in question which demands a radical departure from an analysis based on linearity (such as the Fourier analysis) and which appears to be best treated by the LFD.

Acknowledgements

The author would like to thank M. Glaser and P.V. Akimov for their help in the preparation of the manuscript.

References

Akimov, P.V., Schamel, H., 2002. Space–charge-limited current in electron diodes under the influence of collisions. J. Appl. Phys. 92, 1690.

Akimov, P.V., Schamel, H., Ender, A.Ya., Kuznetsov, V.I., 2003. Switching as a dynamical process in electron diodes. J. Appl. Phys. 93, 1246.

Akimov, P.V., Schamel, H., Kolinsky, H., Ender, A.Ya., Kuznetsov, V.I., 2001. The true nature of space–charge-limited currents in electron vacuum diodes: a Lagrangian revision with corrections. Phys. Plasmas 8, 3788.

Belova, N.G., Galeev, A.A., Sagdeev, R.Z., Sigov, Yu.S., 1980. Collapse of the electric field in double layers. Soviet Phys. JETP 31, 518.

Bohr, T., Jensen, M.H., Paladin, G., Vulpiani, A., 1998. Dynamical systems approach to turbulence. Nonlin. Sci. Ser. 8, ch. 8, pp. 261 ff.

Child, C.D., 1911. Discharge from hot CaO. Phys. Rev. 32, 492.

Ehler, A.W., 1975. High-energy ions from a CO_2 laser-produced plasma. J. Appl. Phys. 46, 2464.

Ender, A.Ya., Kolinsky, H., Kuznetsov, V.I., Schamel, H., 2000. Collective diode dynamics: an analytical approach. Phys. Rep. 328, 1.

Fay, C.E., Samuel, A.L., Shockley, W., 1938. On the theory of space charge between parallel plane electrodes. Bell Syst. Tech. J. 17, 49.

Galeev, A.A., Sagdeev, R.Z., Shapiro, V.D., Shevchenko, V.I., 1981. The nonlinear theory of the Buneman instability. Soviet Phys. JETP 54, 306.

Godfrey, B.B., 1987. Oscillatory nonlinear electron flow in a Pierce diode. Phys. Fluids 30, 1553.

Gurbatov, S.N., Malakhov, A.M., Saichev, A.I., 1991. Nonlinear random waves and turbulence in nondispersive media: waves, rays, particles. Manchester University Press, Manchester.

Haller, G., 2001. Distinguished material surfaces and coherent structures in three-dimensional fluid flows. Physica D 149, 248.

Karimov, A.R., Schamel, H., 2001. Influence of initial velocity field on the formation of coherent structures in simple hydrodynamic flows. Phys. Plasmas 8, 1180.

Karimov, A.R., Schamel, H., 2002. Singular flow dynamics in three space dimensions driven by advection. Phys. Plasmas 9, 811.

Kolinsky, H., Schamel, H., 1994. Finite ion velocity effects on the stability of Pierce-like diodes. Phys. Plasmas 1, 2359.

Kolinsky, H., Schamel, H., 1995. Counterstreaming electrons and ions in Pierce-like diodes. Phys. Rev. E 52, 4267.

Kolinsky, H., Schamel, H., 1997. Arbitrary potential drops between collector and emitter in pure electron diodes. J. Plasma Phys. 57, 403.

LaPorta, A., Voth, G.A., Crawford, A.M., Alexander, J., Bodenschatz, E., 2001. Fluid particle accelerations in fully developed turbulence. Nature 409, 1017.

Lamb, H., 1932. Hydrodynamics. Cambridge University Press, Cambridge.

Langmuir, I., 1923. The effect of space charge and initial velocities on the potential distribution and thermionic current between parallel plane electrodes. Phys. Rev. 21, 419.
Mantei, T.D., Doveil, F., Gresillon, D., 1976. The large density electron beam–plasma Buneman instability. Plasma Phys. 18, 705.
Ottino, J.M., 1990. Mixing, chaotic advection, and turbulence. Annu. Rev. Fluid Mech. 22, 207.
Pierce, J.R., 1944. Limiting current in electron beams in the presence of ions. J. Appl. Phys. 15, 721.
Sack, Ch., Schamel, H., 1987. Plasma expansion into vacuum—a hydrodynamic approach. Phys. Rep. 156, 311.
Schamel, H., Bujarbarua, S., 1993. Lagrangian description of ion dynamical effects in plasma diodes. Phys. Fluids B 5, 2278.
Schamel, H., Hassan, I.O., 1997. Two wave collapses and a strange soliton in current carrying plasmas. Physica D 105, 253.
Schamel, H., Karimov, A.R., 2000. Collapses of density and vorticity by convection in simple two-dimensional flows. Phys. Plasmas 7, 2790.
Schamel, H., Maslov, V., 1993. Ion dynamical effects in the Pierce diode problem. Phys. Rev. Lett. 70, 1105.
Schamel, H., Maslov, V., 1999. Langmuir wave contraction caused by electron holes. Phys. Scr. T82, 122.
Shandarin, S.F., Zel'dovich, Ya.B., 1989. The large-scale structures of the universe: turbulence, intermittency, structures in a self-gravitating medium. Rev. Mod. Phys. 61, 185.
Takeda, Y., Inuzuka, H., Yamagiwa, K., 1995. Observations of Buneman modes as precursory phenomena of a solitary potential pulse. Phys. Rev. Lett. 74, 1998.
Wu, J., Keolian, R., Rudnick, I., 1984. Observation of a nonpropagating hydrodynamic soliton. Phys. Rev. Lett. 52, 1421.
Yeung, P.K., 2002. Lagrangian investigations of turbulence. Annu. Rev. Fluid Mech. 34, 115.